Biochemical sensing with macrocyclic receptors

Chem Soc Rev

Biochemical sensing with macrocyclic receptors

Journal:	*Chemical Society Reviews*
Manuscript ID	Draft
Article Type:	Review Article
Date Submitted by the Author:	n/a
Complete List of Authors:	Pinalli, Roberta; Universita di Parma, Department of Chemistry, Life Science and Environmental Sustainability Pedrini, Alessandro; Universita di Parma, Department of Chemistry, Life Science and Environmental Sustainability Dalcanale, Enrico; Universita di Parma, Department of Chemistry, Life Science and Environmental Sustainability

Note: The following files were submitted by the author for peer review, but cannot be converted to PDF. You must view these files (e.g. movies) online.

Figure01.rar
Figure02.rar
Figure03.rar
Figure04.rar
Figure05.rar
Figure06.rar
Figure07.rar
Figure08.rar
Figure09.rar
Figure10.rar
Figure11.rar
Figure12.rar
Figure13.rar
Figure14.rar
Figure15.rar
TOC.rar

Journal Name

ARTICLE

Biochemical sensing with macrocyclic receptors

Roberta Pinalli, [a] Alessandro Pedrini [a] and Enrico Dalcanale [a,*]

Received 00th January 20xx,
Accepted 00th January 20xx

DOI: 10.1039/x0xx00000x

www.rsc.org/

Preventive healthcare asks for the development of cheap, precise and non-invasive sensor devices for the early detection of diseases and continuous population screenings. The actual techniques used for diagnosis, e.g. MRI and PET, or for biochemical marker sensing, e.g. immunoassays, are not suitable for continuous monitoring since they are expensive and prone to false positive responses. Synthetic supramolecular receptors are offering new opportunities for the creation of specific, selective and cheap sensor devices for biological sensing of specific target molecules in complex mixture of organic substances. The fundamental challenges to be faced in developing such devices are the precise transfer of the molecular recognition events at the solid-liquid interface and its transduction into a readable signal. In this review we present the progresses made so far to turn synthetic macrocyclic hosts, namely cyclodextrins, calixarenes, cucurbiturils and cavitands, into effective biochemical sensors and the strategies utilized to solve the above mentioned issues. The performances of the developed sensing devices based on these receptors in detecting specific biological molecules, drugs and proteins are critically discussed.

1. Introduction

The quest for biochemical sensors has its roots in preventive healthcare, i.e. the use of cheap, non-invasive devices for the screening of population targeted at the early detection of diseases. The social and economic benefits for society of this endeavour is clearly sketched in Figure 1 in the case of breast cancer.[1] As can be clearly seen from Figure 1, survival rates and treatment costs are inversely related, making of paramount importance the early detection of cancer both for the survival of patients and for reducing the costs of national medical services. So far, the most reliable approaches to detect cancer rely on medical imaging using techniques like Computed Tomography (CT), Magnetic Resonance Imaging (MRI) and Positron Emission Tomography (PET).[2] These diagnostic tools require costly instrumentation and specialized personnel, which make them too expensive for large population screenings. Moreover, they suffer of the presence of a sizable number of false positive responses, which lead to unnecessary biopsies of potentially carcinogenic nodules. The alternative solution to reduce morbidity and mortality among population is finding a reliable biochemical marker, specific for a given disease. Once the marker has been found and validated as diagnostic, the problem becomes its detection in biological fluids like blood or urine, usually in very low concentration. Here sensing comes into play, in the form of cheap, non-invasive devices amenable to be used in screenings. Over the past few decades the detection of biochemical markers has been mainly based on immunological

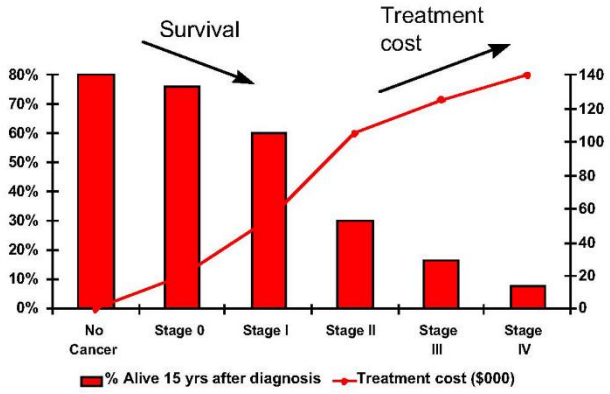

Figure 1. The burden of cancer. Survival rate and treatment costs at the different stages of breast cancer diagnosis. American Cancer Society. Cancer Facts & Figures 2009.

techniques, because antibodies offer unrivalled specificity, particularly when the analytes are large molecules like proteins.[3] Strictly speaking, immunoassays are dosimeters not sensors, since they lack reversibility. Therefore, they are not amenable for continuous monitoring. Moreover, they are often expensive, unstable, and cannot be prepared for some types of analytes. Typical problems encountered with antibodies are poor batch-to-batch reproducibility[4] and reduced selectivity between similar analytes, like the mis-identification of epitopes.[5]

In the cases where these drawbacks are crucial, alternative solutions must be considered. In this context, supramolecular chemistry offers a wide choice of synthetic receptors tuned for binding a large number of analytes, ranging from simple ions to complex organic molecules. Macrocycles like cyclodextrins, calixarenes, cucurbiturils and cavitands are the workhorses of synthetic receptors, featuring excellent molecular recognition properties for a large and diverse pool of guests. All these

[a] *Department of Chemistry, Life Science and Environmental Sustainability, University of Parma, Parco Area delle Scienze 17/A, 43124 Parma, Italy.*

† Footnotes relating to the title and/or authors should appear here.
Electronic Supplementary Information (ESI) available: [details of any supplementary information available should be included here]. See DOI: 10.1039/x0xx00000x

classes of compounds have in common the presence of an enforced cavity of molecular dimensions which acts as molecular recognition site for the incoming analytes. Their molecular recognition properties are generally well-studied both in terms of analytes of interest and interferents. The cavity size and shape as well as type, number and directionality of the interactions can be tuned according to the principles of complementarity for structural recognition and preorganization to provide binding power. In most cases they are chemically stable, easy to functionalize, available in high purity and in substantial quantities. With both the synthetic and molecular recognition toolboxes filled, macrocyclic receptors are amenable to be designed and prepared according to the analytical problem to be solved. Their decoration with fluorescent, chemoluminescent or electrochemical tags is a common way to turn them into so called "molecular probes". However, as clearly pointed out by O. S. Wolfbeis,[6] molecular probes are not sensors. Sensors are solid state devices operating at the gas-solid or gas-liquid interface. The molecular receptors must be therefore employed in the solid state, in the form of a thin film, a monolayer, embedded in a polymer matrix or grafted on surfaces. This evidence brings in the issue of moving molecular recognition from solution to interfaces. The mere presence of a molecular receptor in the sensitive layer of a sensor does not guarantee sensing selectivity. Two bottlenecks are hindering the exploitation of synthetic receptors in biochemical sensing, namely, the precise transfer of the intrinsic molecular recognition properties at the water-solid interface and the high fidelity transduction of the interfacial molecular recognition events into a readable signal. More often than not the matrix to be analysed is not water, but a water –based fluid containing a complex mixture of organic substances and salts, which exacerbates the problem.

The present review covers the efforts made so far to turn macrocyclic receptors into effective biochemical sensors and the strategies utilized to overcome the above mentioned bottlenecks. It is organized per receptor class, focusing on the four major classes of macrocycles which has been turned into sensors so far, namely cyclodextrins, calixarenes, cucurbiturils and cavitands. Furthermore, two promising macrocyclic classes of receptors , namely pillarenes and molecular tweezers, have been mentioned even if no sensors have been made with them so far.

2. Cyclodextrins

β-Cyclodextrin (β-CD) is a naturally occurring torus-shaped cyclic oligosaccharide presenting a central hydrophobic cavity that allows the enclosure of several types of lipophilic guest molecules of appropriate size and shape. The cavity of β-CD is lined up with 21 hydroxyl groups, which impart a highly hydrophilic character to the external part of the molecule. This compartmentalised amphiphilic character is pivotal for the use of β-CD in biochemical sensors.[7]

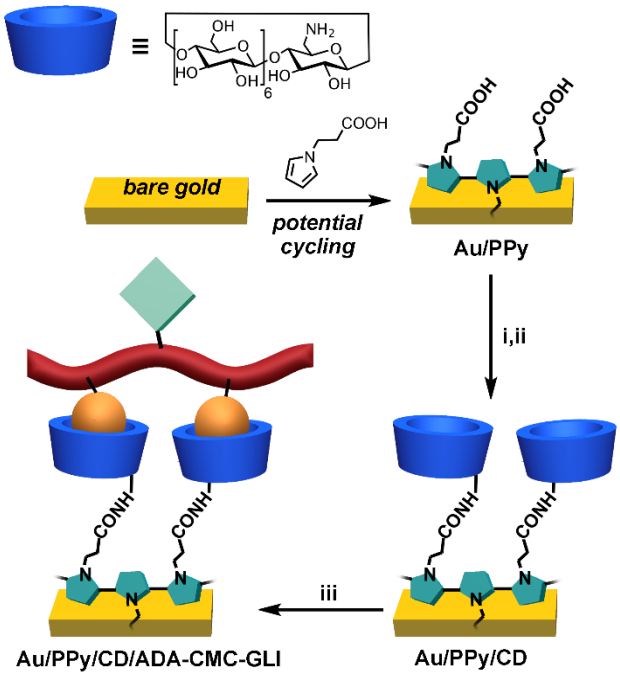

Figure 2. Functionalization of the gold biosensor surface. (i) EDC/NHS; (ii) mono-6-amino-6-deoxy- β-CD; (iii) ADA-CMC-GLI. Adapted from reference 9.

The construction of CD-based biosensors requires the engineering of the transducer surface to accommodate the CDs with the correct orientation of the functional groups. Among the sensor platform, electrochemical sensors are very convenient devices, simple to design, ensuring reversible and reproducible measurements, as well as precise and accurate analytical information. Accordingly, CDs have received increasing interest as components of selective layers of many electrochemical sensors.[8]

2.1 Electrochemical sensors for antibody detection

A novel approach to modify gold surfaces with an electropolymerized pyrrole-cyclodextrin film for the construction of high-performance biosensors for antibodies was presented by Fragoso and collaborators in 2016.[9] A β-CD decorated polypyrrole was used as support on disposable screen-printed electrodes (SPE) for the immobilization of a functionalised polysaccharide carrying both adamantanes as CD guests,[10] and gliadin units for antibodies binding. The electrical and optical properties of polypyrroles were coupled with the selectivity provided by the CD hosts to obtain functionalized surfaces with precise molecular recognition properties.

The functionalization approach, presented in Figure 2, is entirely conducted at the solid-liquid interface. Initially, 1H-pyrrole-1-propanoic acid (PyCOOH) was electropolymerized onto the gold surface of SPE through cyclic voltammetry to form a polypyrrole film. The obtained electrodes were then reacted with *N*-(3-dimethylaminopropyl)-*N*'-ethylcarbodiimide hydrochloride (EDC) and *N*-hydroxysuccinimide (NHS) to obtain the corresponding activated esters, which were then reacted with an excess of mono-6-amino-6-deoxy-β-cyclodextrin to

covalently attach the β-CD to the functionalized gold surface. The Au/PPy/CD electrode was incubated into a solution of adamantane-containing carboxymethyl cellulose polymer (ADA-CMC) conjugated to gliadin (ADA-CMC-GLI). The stability of the resulting layer is assured by the multivalency of the host-guest interactions.[11] The last incubation steps with target anti-gliadin antibody and reporting anti-mouse-HRP conjugate were carried out immediately prior to the amperometric measurements. The surface functionalization was confirmed through SPR analyses, cyclic voltammetry and impedance spectroscopy after each modification step. Impedance spectroscopy was also employed to assess the reproducibility of the electropolymerization and ADA-CMC-GLI deposition, since the preparation of reproducible surfaces is essential for practical applications. The resistance to charge transfer value of 16 individual modified working electrodes was measured for each of the electrodes, resulting in a standard deviation of 4.3%. The performance of the resulting amperometric sensor was tested to detect an anti-gliadin antibody by monitoring the formation of a tertiary immunocomplex between the gliadin units immobilized on the ADA-CMC-GLI polymer, the target antibody and a reporter anti-mouse-HRP conjugate. A control device was prepared by immobilizing gliadin on a SAM of 3-mercaptopropionic acid, lacking both PPy and β-CD moieties. Very good sensitivities and low LOD values were obtained only for the sensor presenting CD/ADA interface, demonstrating that this interface plays a crucial role in the antibody detection. The developed biosensor is effective in the amperometric detection of the target antibody in a complex matrix like foetal calf serum containing different amounts of anti-gliadin antibody with signal recovery near 100%.

2.2 Electrochemical sensors for DNA detection

A novel electrochemical sensing strategy for the sensitive detection of target DNA and miRNA was recently proposed by Diao *et al*.[12] The method is based on the combination of the cyclic cleavage reaction of Mg^{2+}-dependent deoxyribozyme, also called DNAzyme, and the host–guest inclusion between ferrocene-labelled hairpin probe (H-1) and nitrogen-doped reduced graphene oxide/β-CD polymer (NRGO/β-CDP) nanocomposites (Figure 3). β-CD polymer, generated by the cross-linking reaction between β-CD and epichlorohydrin (EP),[13] combines high water solubility and recognition capability toward selected guest molecules.[14] The obtained NRGO/β-CDP nanocomposites combine the superior electrocatalytic activity of NRGO, with the molecular recognition properties of β-CDP. Mg^{2+}-dependent DNAzyme generally consists of an enzymatic and a substrate sequence paired to each other, which is cleaved in presence of Mg^{2+} as cofactor to perform the catalytic activity. During multiple turnovers, one Mg^{2+}-dependent DNAzyme can generate the split of a great number of substrates without losing its binding ability or activity, leading to the significant signal amplification for sensitive detection.

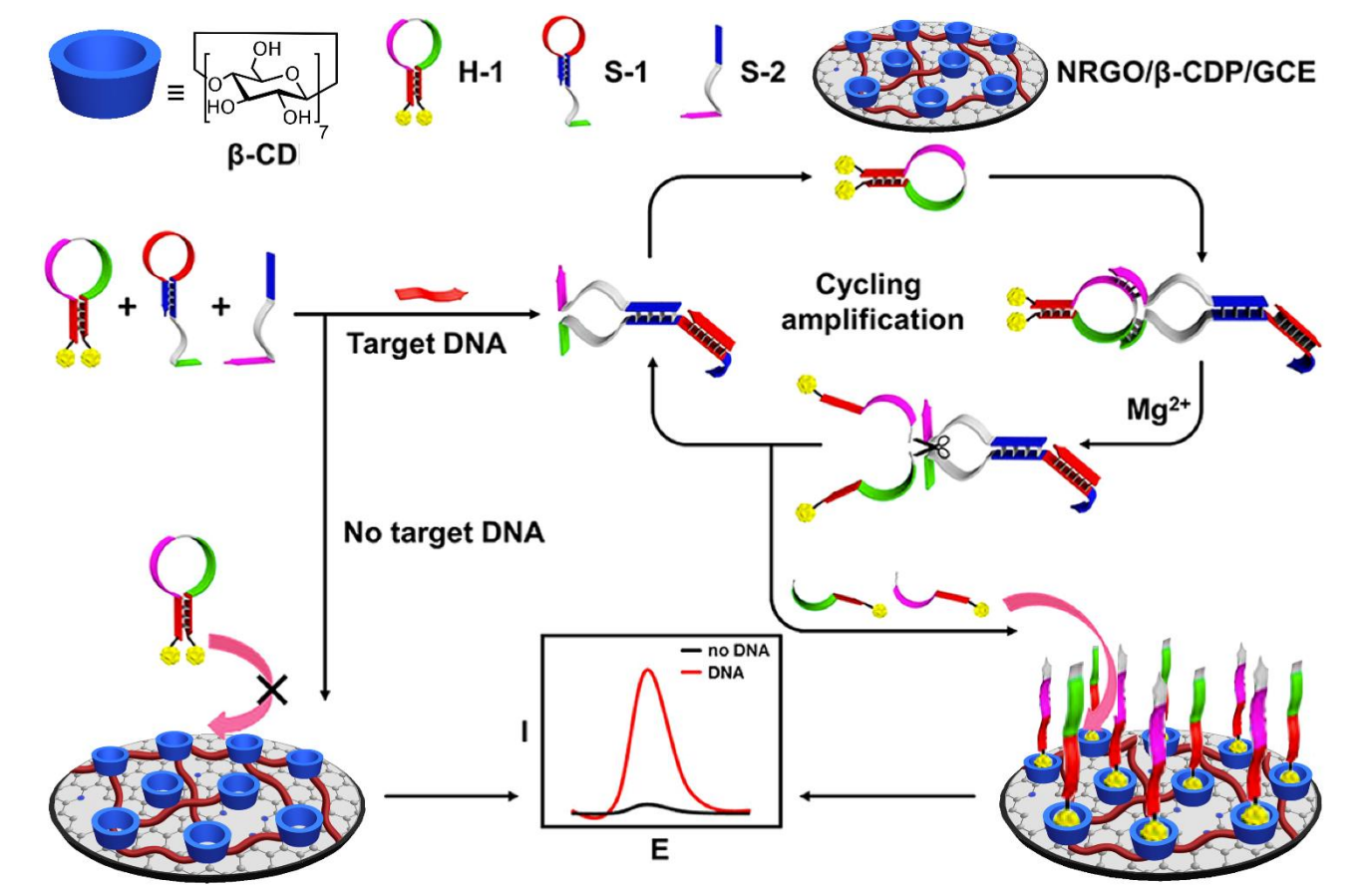

Figure 3. Electrochemical DNA biosensor based on the host–guest interaction and Mg^{2+}-assistant DNA recycling. Adapted from reference 12.

In the absence of target, the hybridization reaction of the stem domain of subunit DNA (S-1) inhibits the formation of Mg^{2+}-dependent DNAzyme. Consequently, the uncleaved hairpin probe (H-1) is incidentally recognized by the β-CDP on the electrode because of dimension matching of the two closely associated ferrocenes, leading to a weak current response. On the contrary, in presence of the target sequence S-2, the hairpin structure of S-1 is opened, giving rise to the active DNAzyme structure that catalyses the cleavage of H-1, due to the synergistic binding of H-1 in the presence of cofactor Mg^{2+}. In this way, the dual-labelled H-1 is divided into two single-stranded oligonucleotides, that are recognize by the β-CDP on the electrode generating an increase of peak current. Each activated DNAzyme undergoes to several recycles to achieve an amplified electrochemical signal for the target. The calculated detection limit was 3.2 fM, at a signal-to-noise ratio of 3 (S/N = 3). The high electrocatalytic activity of NRGO, combined with superior recognition capability of β-CDP toward ferrocene, and excellent cleavage reaction of Mg^{2+}- dependent DNAzyme, render this sensor one of the best for DNA analyses. Furthermore, the Authors demonstrated the efficiency of the proposed method also for the detection of target miRNA, with a concentration range from 50 fM to 0.5 nM. The detection limit was estimated to be 18 fM (S/N = 3), which is much lower than other similar miRNA biosensors present in literature.[15]

The constructed biosensor presents satisfactory fabrication reproducibility, storage stability and selectivity. In particular, the selectivity was demonstrated comparing the current intensity of DNA target to that of single-base and two base mismatched DNA. Only the target DNA gave rise to a significant current enhancement, demonstrating sufficient selectivity to distinguish between the analyte and base mismatched sequences. Finally, the practical application of the developed analytical platform by the determination of target DNA in human serum samples was tested. An acceptable signal recovery with a good relative standard deviation for 5 measurements was obtained for the serum samples spiked with target DNA at different levels. Overall the proposed biosensor presents acceptable accuracy and recovery for DNA detection in clinical diagnosis.

Interesting examples reporting the use of electrochemical biosensors based on β-CD decorated graphene oxide were presented by Huang[16] and Hong.[17] The first Author developed an amperometric enzyme biosensor based on reduced graphene oxide (RGO) modified with β-CD for dopamine detection. Dopamine is an important neurotransmitter, which plays important roles in central nervous, cardiovascular and endocrine systems.[18] Different approaches, mainly spectrophotometric[19] and electrochemical,[20] have been exploited for the rapid and sensitive detection of dopamine for diagnostic applications. Among these methods, the electrochemical approach has emerged as promising for dopamine quantitative determination thanks to its easy operation, low cost, fast response and feasibility of miniaturization.[21] RGO can interact with organic molecules thanks to the presence of structural defects, such as hydroxyl and epoxy groups on the basal plane and carboxylic acid groups at the edge sites.[16] The functionalization of RGO with β-CD generates a material with large surface area, high conductivity, and molecular recognition properties at the solid-water interface. Moreover, the presence of β-CD on the RGO surface provides a friendly microenvironment for retaining enzymatic activity.[16]

Huang and collaborators[16] exploited laccase to develop a biosensor for dopamine determination. Laccase is a protein known to establish attractive electrostatic interactions with the positively charged dopamine.[22] In detail, an inclusion complex between β-CD and benzaldehyde was formed in water. The β-CD-laccase complex was prepared by reacting the aldehyde moiety with the N-terminus of laccase forming an imine bond. This complex was then anchored onto a RGO modified SPE via esterification of the RGO carboxylic groups with β-CD hydroxyl units. The developed biosensor showed good stability and performed selective determination of dopamine in phosphate-buffered saline (PBS) diluted human urine samples in the presence of high concentration of aspartic acid, one of the main interferents.

Recently, Hong and co-workers developed a sandwich-type electrochemical immunosensor for the simultaneous detection of two cancer markers, namely carcinoembryonic antigen (CEA) and alpha-fetoprotein (AFP).[17] The sensor is composed by graphene oxide functionalized with gold nanoparticles (GO–AuNPs) to enhance the sensitivity of the electrochemical sensor substrates, onto which anti-CEA and anti-AFP antibodies are immobilized as anti-CEA•CEA and anti-AFP•AFP complexes. Graphene oxide functionalized with the complex β-CD–Ferrocene-anti-CEA (GO–CD–Fc-anti-CEA) and Cu_2O–GO–CD-anti-AFP are deposited onto the functionalized sensor platform as distinguishable signal probes. The main advantages of the immunosensor can be resumed as follows: (i) GO–AuNPs immobilize primary antibodies without deactivation, (ii) the large amount of CD deposited on the GO surface increases the water solubility of graphene overcoming the aggregation of reduced graphene oxide, and forms host-guest inclusion complexes with redox probes, thus preserving good activity, (iii) the simultaneous detection of CEA and AFP provides reliable output for the diagnosis and early detection of cancer. The performance of the proposed immunosensor was tested in real blood or tissue samples, and it showed acceptable stability, high sensitivity, a wide linear range and detection limits in the ppb range, thus revealing potential for the simultaneous detection of multianalytes in clinical diagnosis and screening.

The role of CDs in all these sensors is to act as anchoring point of the real receptors through non-covalent inclusion within the cavity, given the fact that themselves are not sufficiently selective for the purpose.

3. Calix[n]arenes

Calix[n]arenes chemistry is so well developed that they can be easily functionalized at either the upper and lower rim to tailor their recognition properties towards a desired class of analytes, as well as to integrate them in all the major transduction platforms. Guests complexation highly depends on receptor dimensions, that can be set choosing the proper number of monomeric units ($4 < n < 8$), and multiple non-covalent interactions involved, such as hydrogen bonding, π-π stacking, cation-π and CH-π interactions.[23,24] Moreover, calix[n]arenes conformation can be kept mobile to exploit an induced-fit binding, or, in contrast, finely locked in preorganized structures for a more specific binding. Their ability to bind a wide range of biomolecules, such nucleic acids, amino acids, Active Pharmaceutical Ingredients (API), peptides and proteins has been extensively studied.[25,26] Such recognition properties have been successfully exploited to promote proteins immobilization on surface, the use of calixarenes as carriers through membranes, as well as their incorporation into channelling systems.[27] Calix[n]arene-based sensing of biological substances relies mainly on spectroscopic and electrochemical techniques.

3.1 Fluorescence-based sensing of epigenetic histone modifications

There are over 60 different residues on histones where modifications have been detected either by mass spectrometry or by specific antibodies. In particular, the latter are the dominant tools for the identification of post-translational modifications (PTMs) even if antibody-based assays suffer from high batch-to-batch variability. At least 25% of most commercially available histone-modification antibodies have substantial problems of specificity or utility and they needed to be tested independently.[4] In this field the development of assays based on synthetic receptors is particularly attractive, as batch-to-batch and lab-to-lab reproducibility might be improved using chemicals that can be purified to homogeneity.

For this application, fluorescent-based sensing has grown dramatically after the availability of water soluble anionic calix[n]arenes.[28] In particular, dye displacement assays based on *p*-sulfonatocalix[n]arenes have attracted considerable attention since they can be employed in aqueous and physiological solutions with a variety of dyes. Chemical sensor arrays with partially selective receptors, such as sulfonato calixarenes, have been attracted increasing interest after the seminal work reported by Hof and co-workers.[29] The Authors presented a mix and match toolkit of readily available dyes and calixarene host molecules that can be combined to form dye-displacement sensors for *in vitro* detection of a wide variety of cationic peptides. In the displacement scheme used, the fluorescent dye is quenched when complexed by the calixarene host, and active when a competitive guest displaces the dye from the cavity (Figure 4).

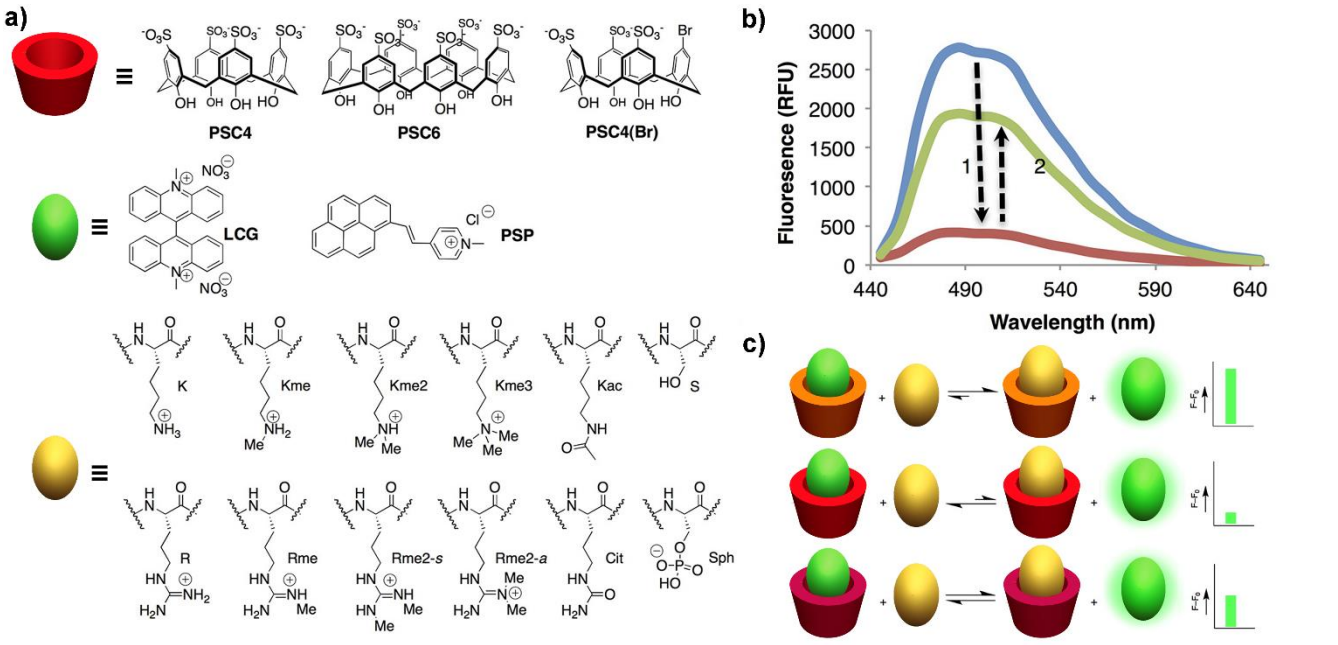

Figure 4. a) Structures of post-translationally modified residues, hosts and fluorescent dyes used in this study; b) The principle of the fluorescent response is provided with representative data from a single sensor + analyte combination: the emission of a fluorescent dye (blue trace) is quenched upon addition of anionic host (red trace, step 1) and then restored to some extent upon addition of analyte (green trace, step 2) to produce a signal in the form of F − Fo. Conditions: phosphate buffer, 10 mM, pH 7.4; [LCG] = 0.5 μM; [PSC4] = 1.5 μM; [Kme3] = 200 μM; c) Illustration of the principle of using patterns of data produced by chemical sensor arrays to identify and quantify analytes. Adapted from reference 29.

Journal Name

ARTICLE

Two distinct types of sensor arrays were developed, namely Type 1 and Type 2, using two different calixarenes as common building blocks. "Type 1" array employs a single calixarene host (*p*-sulfonatocalix[6]arene, PSC6) in all sensor elements and 1-methyl-4-(2-pyren-1-yl-vinyl)-pyridinium chloride (PSP) as dye. The different fluorescent responses for different analytes are based on the variation of pH and/or organic co-solvent conditions. "Type 2" array uses different calixarene hosts (PSC6, PSC4, and PSC4(Br)) for each element of the sensor array and bis-N-methyl acridinium nitrate (LCG) as dye. This dye does not require organic co-solvents,[30] and only pure, buffered water is used in the working conditions. The experimental set consisted in two parts: (i) a 96-well plate where sensor array components (dye, calixarene, buffer, solvent) and analytes were mixed, and (ii) a fluorescent plate reader. The fluorescence emission value at λ_{max} was considered.

Initial proof-of-concept studies involved the discrimination of a set of closely related modified lysines (R, K, Kac, Kme, Kme2, and Kme3; Figure 4a) that cannot be distinguished by conventional, single-sensor dye displacement due to their very similar structures and/or charge states at neutral pH. The "Type I" array produced unique sets of fluorescent responses for this set of guests based on to the peculiar affinities of the analytes for the host at different pH values. The fluorescence responses were treated through linear discriminant analysis (LDA)[31] to convert the multivariable raw fingerprint data into simple plots expressing the multidimensional variance in a 2D data sets. The confidence level of discrimination was 99%. The Type 2 array, was able to discriminate among this set of amino acid analytes with 90% confidence. In this case the discrimination is not depending on the different analytes' pK_a values but arise from the different affinity of the analytes for each of the three different calixarene hosts used. For Type 2 array even very low fluorescent responses, related to weak binding, are sufficient for discrimination of the analytes. The Type 2 array sensor was then selected to detected synthetic modified peptides. It was able to discriminate mono-, di-, and trimethylation states of lysine in histone 3 (H3) tails without interference from pristine and acetylated lysines.

Finally, the Authors demonstrated that the Type 2 sensor array is able to discriminate also PTM states of arginine in histone 4 tails. Despite the small magnitudes of fluorescence responses, the fingerprint data allowed discrimination of the four related analytes, including the separation between asymmetric and symmetric dimethylated arginines, that differ only by isomeric transposition of a single methyl group from one nitrogen to another on the same arginine side chain. The developed toolkit revealed to be able to report simultaneously on the concentrations and identities of histone modifications. In particular, after the data processing of a simple, two-component sensor array, it was possible to measure and track the conversion of H3 histone tail starting material to two distinct end products representing methylation at two biomedically important sites (H3K4me3 and H3K9me3). These preliminary data suggest that a single sensor array might serve as an *in vitro* readout for dozens or hundreds of enzymes, without the need for antibodies specific to the products of the various enzymatic reactions. The toolkit can be easily expandable to other set of calixarenes and dyes to detect *in vitro* different type of peptides or proteins, like anionic ones. Even if this approach is limited to *in vitro* analysis and requires higher analyte concentration compered to antibodies, it is cheaper than biological assays and represents a promising application of host-guest recognition to epigenetic research.

3.2 Lipid membranes as selective layer for protein sensing

An alternative approach to fluorescence-based detection of amino acids and proteins with calix[n]arenes receptors was proposed by Schrader and co-workers in 2005.[32] Taking inspiration from natural recognition processes occurring at lipid membrane interfaces, the Authors developed a sensing platform constituted by lipid monolayer doped with a small amount of molecular receptors that interact with protein surfaces leading to detectable monolayer expansion.

Binding experiments of calix[4]arene tetraphosphonate (Figure 5a, **1**) were carried out in free solution with various arginine and lysine derivatives to determine association constants, stoichiometries and complex geometries prior to investigating the complexation in a monolayer. The progressive incorporation of receptor molecules in the stearic acid monolayer upon addition of different aliquots of calix[4]arene tetraphosphonate was evidenced by regular shifts in the pressure/area diagram. Given their strongly amphiphilic nature, tetraphosphonate calixarenes orient their cavities toward water, without showing any self-association at the concentrations involved. Subsequent injection of basic amino acids into the aqueous subphase produced moderate, but distinct, additional expansions of the pressure/area diagrams (Figure 5b). As expected, effective complexation of small species does not require monolayer reorganization, but involves mainly calix[4]arene conformational changes. Instead, for the binding of di- and tripeptides several calixarenes must cooperate through multipoint binding. Receptor molecules,

Journal Name

ARTICLE

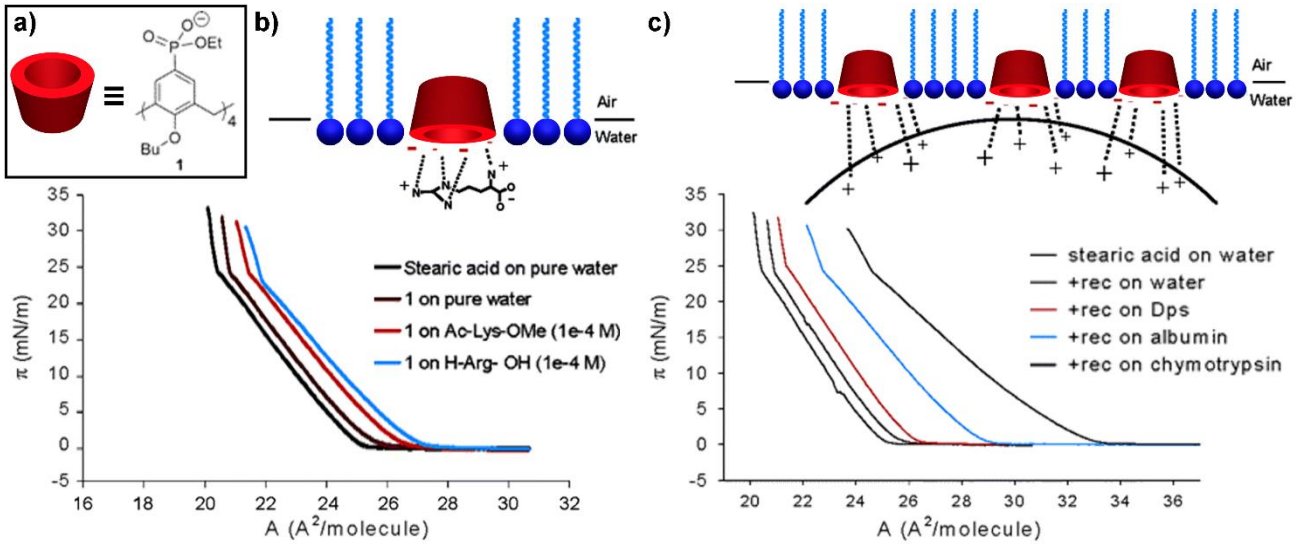

Figure 5. a) Structure of tetraphosphonate calix[4]arene **1**; b) Schematic representation of the calixarene monolayer recognizing an arginine in the subphase (top) and pressure/area isotherms for the embedding of receptor **1** (0.13 equiv) into a stearic acid monolayer, followed by molecular recognition of N/C- protected arginine and lysine (both 10^{-4} M, bottom); c) Proposed binding mode of the embedded calixarene tetraphosphonate **1** with basic proteins in the aqueous subphase (top) and Langmuir isotherms obtained from 0.13 equiv of **1** incorporated into a stearic acid monolayer at the air-water interface, over protein solutions of ~10^{-8} M (bottom). Adapted from reference 32.

which are expected to be surrounded by approximately 200 stearic acid molecules, move through the monolayer and rearrange producing remarkable expansions in the pressure/area diagram, as demonstrated with diarginine and triarginine. This recognition mechanism was further investigated with larger peptides and proteins at concentrations in the nanomolar range (10^{-8} M, Figure 5c). Proteins with negative surfaces, such as Dps dodecamer and albumin, bind much more weakly to the negatively charged calix[4]arene in the monolayer, as demonstrated by the resulting isotherms.

The largest shifts were found for basic proteins with an isoelectric point (pI) higher than 7, such as histone H1 and chymotrypsin. Interestingly, an almost linear correlation was found between the expansion of the monolayer (ΔA_{rec}) and the pI values of the respective proteins.

To exclude a major role of unspecific Coulomb interactions in the recognition process, a number of related anionic amphiphiles were embedded in the same stearic acid monolayer without effects. The platform was extended to the recognition of acidic proteins embedding cationic calix[4]arenes amphiphiles in the lipid monolayer. Calix[4]arene derivative **2**, bearing four pendant benzylammonium groups at the upper rim, and its anilinium counterpart **3** were designed and synthesized for this purpose (Figure 6a). Monolayers doped with the former revealed to be selective for acidic proteins at a concentration of 10^{-8} M, while the latter receptor presented recognition properties toward a wide range of guests varying in size, polarity, and pI. In the case of receptor **3** only a relatively small fraction of the cationic species is fully protonated at neutral pH and both protonated NH_3 groups and free NH_2 amino groups are present at the upper rim of the scaffold, acting as strong hydrogen bond donor and acceptor groups respectively.

Since each protein interacts differently with monolayers doped with receptor units **1**, **2**, **3**, or mixtures thereof, the different responses can lead to a recognition pattern that is specific for each individual protein (Figure 6b). Thus, each column in the graphical representation in Figure 6c constitutes a fingerprint of the respective protein, reflecting its different interactions with anionic (**1**), cationic (**2**), mixed polar (**3**), or zwitterionic (**1+3**) self-assembled monolayers. Taken together, these results pinpoint the possibility to effectively apply calix[4]arene-decorated surfaces to the specific and quantitative detection of peptides and proteins at low concentrations. However, for a real sensing device the deposition of these monolayers on a suitable transduction platform capable of recording the surface changes related to the multipoint recognition is required. Microcantilevers (see section 4.4), operating at the solid-water interface, could do the job by recording and correlating the multipoint protein binding to mechanical deflection.

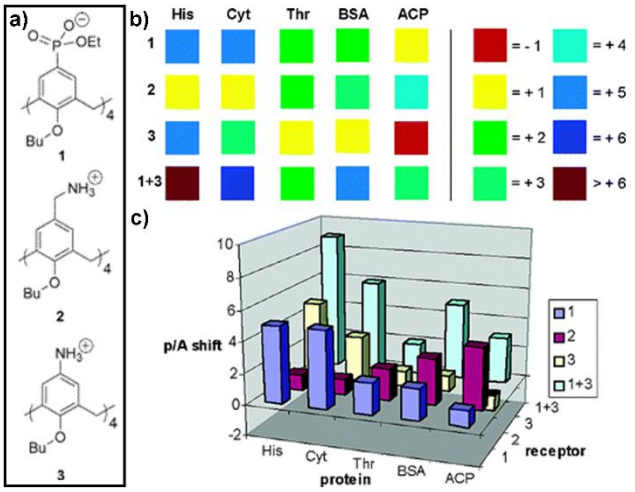

Figure 6. a) Structures of the calix[4]arene-based receptors involved in the study; b) recognition pattern evolving from film balance experiments with five different proteins (histone H1, cytochrome *c*, thrombin, BSA, and ACP) and four different calixarene receptor cocktails (**1**, **2**, **3**, and **1**+**3**). Color coding represents p/A shifts in A^2; c) fingerprints of the five proteins based on the doped monolayer expansion assay (protein concentration: 10^{-8} M). Adapted from reference 32.

3.3 Calixarene-based electrochemical biosensors for the detection of biomolecules

Electrochemical biosensors are valuable devices for food technology, biotechnology, pharmaceutical studies and clinical diagnosis due to their simplicity, low cost, quick response and portability. Several examples of calixarene-based electrochemical biosensors are reported in the literature. Calix[4]arenes were incorporated in freely-suspended and metal supported planar bilayer lipid membranes (BLMs) for the rapid electrochemical detection of catecholamine[33] and adrenaline.[34]

Self-assembled monolayers of calix[4]crown-5 on gold electrodes were applied to the recognition of protonated aliphatic polyamines by electrochemical impedance spectroscopy (EIS).[35] The formation of host-guest complexes on the monolayer promoted or hampered the electron transfer from the electrode to the probe ($Fe(CN)6^{3-/4-}$ pair) depending on the number of ammonium groups and their arrangement in the alkyl chains. The proposed analytical method was tested on simulated urine, blood, erythrocyte, and cerebrospinal fluids containing protonated spermidine.

A calix[4]arene crown-4 ether film modified glassy carbon electrode was fabricated and its electrocatalytic activity in the oxidation of norepinephrine was evaluated by EIS and voltammetric methods.[36] Excellent linear relationships were obtained in two concentration ranges of the analyte allowing the development of a sensitive and selective amperometric method for norepinephrine determination.

An electrochemical sensor for dopamine was based on silver nanoparticles decorated with redox-active thiacalixarene bearing catechol moieties at the lower rim.[37] Nanomolar concentrations of the analyte were detected evaluating its cathodic peak in cyclic voltammetry, generated by the concerted electron transfer between the electrode and dihydroxyphenolic fragment of dopamine, combined with its cyclization and reoxidation within the surface film.

A chiral probe exhibiting a highly selective recognition for amino propanol enantiomers was prepared grafting R-mandelic acid functionalized calix[4]arene on graphene *via* a click reaction.[38] The impedimetric sensor obtained by the deposition of the resulting material on a glassy carbon electrode showed a good response to amino propanol with a detection limit at the nM level in serum.

3.4 Potentiometric sensing of creatinine with calix[4]pyrroles

Calixpyrroles (*meso*-octasubstituted porphyrinogens) are a class of macrocycles deriving from the condensation between pyrrole and acetone in the presence of an acid. The descriptive name “calixpyrrole” was coined by Sessler and co-workers due to the conformational analogy between them and the calix[4]arenes.[39]

In 2016 Ballester and co-workers exploited the recognition properties of a monophosphonate calix[4]pyrrole in the construction of a highly sensitive and selective potentiometric sensor for the determination of creatinine levels in biological fluids.[40] The detection and quantification of creatinine in human urine and blood is clinically relevant, as its level reflects renal, muscular and thyroid functions. The normal levels of creatinine range from 3 to 25 mM in urine and from 0.06 to 0.42 mM in blood. Since common enzymatic or chromatographic methods suffer for practical weakness, the Authors proposed an alternative approach based on ion-selective electrodes (ISEs). These simple and robust ion-concertation gauges, already in use in routine clinical laboratories, can target relatively complex analytes through the proper choice of “ionophores”. A calix[4]pyrrole-based ionophore (Figure 7a, **1**) was designed to host creatinine in its aromatic polar cavity by surrounding most of the guest surface. Moreover, the presence of a single phosphonate group at the open end and four pyrrole NH moieties at the closed end allows the formation of complementary hydrogen-bonding interactions with the polar functions of the included analyte. The complexation abilities of receptor **1** towards creatinine (**2**), and its protonated form, the creatininium cation (**2**·H^+), as tetrakis(3,5-bis(tri-fluoromethyl)phenyl)borate (BARF) salt, were exhaustively investigated in solution through 1D and 2D NMR experiments as well as in the solid state *via* single crystal X-ray diffraction. The bis(methylene)-bridged receptor **3** was taken as reference compound.

Three distinct ISEs, with identical polymeric membrane compositions, were prepared: a “blank” sensor with no embedded ionophores and sensors 1 and 2 containing respectively ionophores **1** and **3**. Polyvinylchloride (PVC) was used as polymeric support, *ortho*-nitrophenyl octyl ether (*o*-NPOE) as plasticizer, with a polymer/plasticizer weight ratio of 1:2, and potassium tetrakis[3,5-bis(trifluoromethyl)phenyl] borate (KBARF) as ion exchanger (30 mol % with respect to the ionophore). The changes in electrical potential for the three sensors upon increasing the concentration of the creatininium cation (**2**·H^+) are reported in Figure 7b. According to the working principle of these electrodes, the electrical potential is

Journal Name

ARTICLE

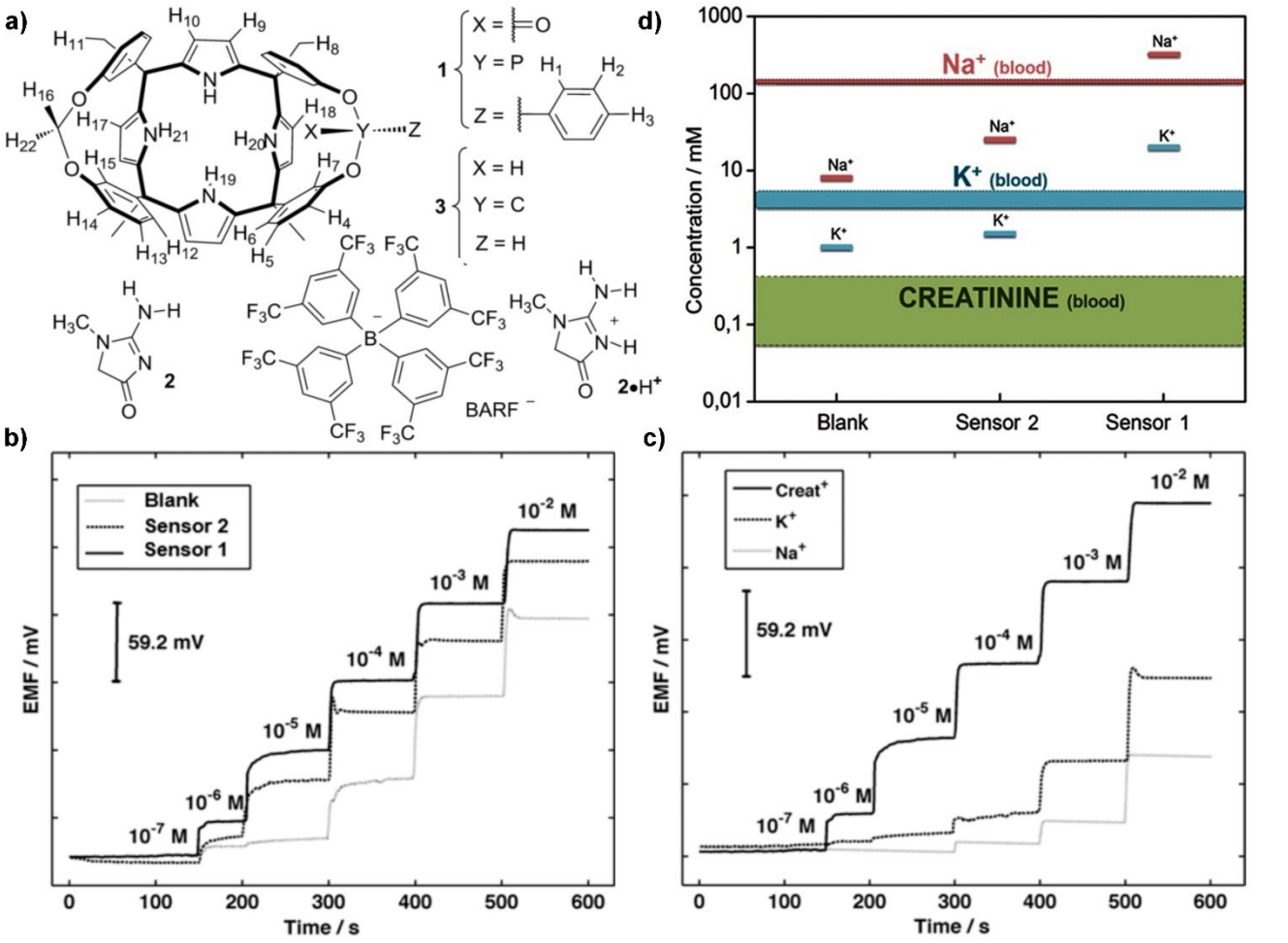

Figure 7. a) Structures of monophosphonate-bridged calix[4]pyrrole (**1**), reference receptor (**3**), creatinine (**2**) and BARF salt of creatininium cation (**2**·H⁺); b) response of the electromotive force (EMF) to incremental changes in the creatininium concentration (**2**·H⁺) for the three different sensors in buffered water solution at pH 3.4; c) response of the EMF of sensor 1 to incremental changes in the concentration of different cations; d) threshold values in units of concentration, corresponding to the maximum allowed concentration of the interferent ions at which the creatinine concentration can still be determined in real samples. Adapted from reference 40.

generated by the partition equilibrium of **2**·H⁺ at the membrane phase boundary and depends on the activity of the creatinine ions ($a_{creatinine}$).

For sensor 1 an ideal response was observed from 1 μM to 10 mM with a LOD of 0.6 ± 0.2 μM, one order of magnitude lower than that recorded by sensor 2 (4.4 ± 0.6 μM). To test the applicability of these ISEs to the analysis of real biological sample, their response to main interferents, such as Na^+ and K^+, was carefully evaluated. The selectivity against inorganic cations is a key challenge for creatinine sensors considering that their presence is by far predominant in biological fluids. The variation of electromotive force (EMF) in sensor 1 for the two inorganic cations was found to be reduced compared to creatininium cation (Figure 7c). Selectivity of the three sensors, calculated from the corresponding calibration curves, were also compared to the most stringent "required selectivity coefficients" and were found to be of 1.9 orders of magnitude lower for K^+ and 3.4 orders of magnitude lower for Na^+ in blood (Figure 7d).

Finally, sensor 1 was tested on real urine and plasma samples from both healthy people and patients with renal dysfunction. Taking advantage of the low limits of detection offered by this sensor, biofouling, the unspecific response caused by the attachment of lipophilic components onto the surface of the polymeric membrane, was successfully minimized by diluting the samples. An excellent linear correlation with a slope close to 1 and an intercept close to 0 was found comparing ISE results to the standard reference method (the Jaffé method), demonstrating the validity of the proposed method for the analysis of creatinine levels in real biological samples.

4. Cavitands

Cavitands are a class of resorcinarene-based abiotic receptors having enforced cavities of molecular dimensions.[41] In the design of cavitands, the choice of the bridging groups connecting the phenolic hydroxyls of the resorcinarene scaffold is pivotal, since it determines shape, rigidity, dimensions and complexation properties of the resulting cavity. Besides shape complementary, the selective binding of a guest by a cavitand receptor requires the presence of specific weak interactions such as hydrogen bonding,[42] π-π stacking,[43] and CH-π[44] and cation-π interactions.[45] The functionalization of the lower rim of cavitands is functional to surface grafting. Among the many different classes of cavitands reported in the literature, tetraphosphonate, octamide and tetracarboxylate ones are those employed for biochemical sensing so far.

4.1 Conductimetric and ECL sensing of sarcosine with tetraphosphonate cavitands

Tetraphosphonate cavitands (Tiiii)[46] show notable molecular recognition properties towards *N*-methyl ammonium salts both in the liquid,[47,48,49] and in the solid state.[50,51] The origin of the receptor selectivity towards mono methylated ammonium salts, derives from the presence of three synergistic interaction modes: (i) N^+•••O=P cation–dipole interactions; (ii) cation–π interactions of the acidic $^+N–CH_3$ group with the π basic cavity;[45] (iii) two simultaneous hydrogen bonds between two adjacent P=O bridges and the two nitrogen protons. Within the ammonium salt series, the preference of the receptor for the mono-methylated species over di- and tri-methylated ones is determined by the number of H-bonds formed, while non-methylated ammonium ions are less complexed by the lack of cation-π interactions.[51] This peculiar affinity of tetraphosphonate cavitands toward the H_2N^+-CH_3 group makes these receptors particularly suited for the detection of a broad range of biologically active compounds containing this residue, like synthetic drugs[52,53] and biomarkers.[54]

A comprehensive study on the complexation properties of Tiiii toward mono-methylated amino acids[55] revealed that, upon moving from methanol to water, the complex formation changes from an enthalpy–entropy driven process to an enthalpy driven-entropy opposed process. In particular, the K_a value decreases by 3 orders of magnitude (from 10^6 to 10^3) in moving from methanol to water. However, this drop is associated to complete specificity since in aqueous solutions *N*-methylated amino acids are exclusively complexed.

Abnormal quantity of sarcosine, also known as *N*-methylglycine, in urine has been linked to early stage detection of aggressive prostate cancer.[56] The challenge of detecting sarcosine in urine *via* molecular recognition is mainly due to the presence of overwhelming amounts of potential interferents such as glycine, ammonium, sodium, potassium, magnesium, and calcium salts.

The first sensing device for the detection of sarcosine in the urine based on tetraphosphonate cavitands decorating single-walled carbon nanotubes (SWCNTs), was reported by Dalcanale and Swager in 2012.[57] Carbon nanotubes are a very sensitive and versatile platform for sensor engineering, thanks to their electrical properties and quasi-one-dimensional structure,[58] but they lack selectivity.[59,60] To overcome this drawback, Tiiii was covalently attached onto SWCNTs surface (Tiiii•SWCNTs). The molecular recognition abilities of Tiiii•SWCNTs at the solid-water interface were assessed *via* XPS and through ^{31}P MAS NMR, using 4-bromo-*N*-methyl butyl ammonium bromide as reference guest (**1**, Figure 8a). After exposure of the functionalized SWNTs to an aqueous solution of **1**, the XPS spectrum showed the appearance of the diagnostic bromine signal (Figure 8b), while the ^{31}P MAS NMR showed the shift of the P signal due to complexation. The reversibility of the process was checked by breaking the cavitand-guest complex via deprotonation of the guest with 1,8-diazabicyclo[5.4.0]undec-7ene (DBU).[61] After the deprotonation step ^{31}P MAS NMR recorded the spectrum of the pristine Tiiii•SWCNTs, confirming the successful removal of the guest.

The corresponding conductimetric sensor was prepared by drop casting Tiiii@SWCNTs onto a glass slide decorated with two Au electrodes. The device detects selectively sarcosine over glycine (guests **2** and **3** Figure 8d), and tetraethyl ammonium chloride (guest **4**), this last one too bulky to be complexed.[51] Interestingly, the exposure of the device to the target guest **2** at pH 5 resulted in an increase in current, while exposure to interferents **3** and **4** led to a current decrease (Figure 8c,f). This different behaviour in the current change upon exposure to the guests (positive in one case and opposite for the controls), allows selective detection of the analytes, regardless of their concentration. The covalent functionalization of the cavitand onto the SWCTNs led to a SWCNTs-based device with high stability, since no significant change in sensitivity was observed over several months of regular operation, and sensitivity, as the detection limit for sarcosine resulted to be 0.02 mM (Figure 8e). Unfortunately, upon moving from water to urine, the device failed to detect exclusively sarcosine, since the inorganic cations present in urine interact directly with the SWCNTs, leading to a current change which cover the sarcosine response.

Journal Name

ARTICLE

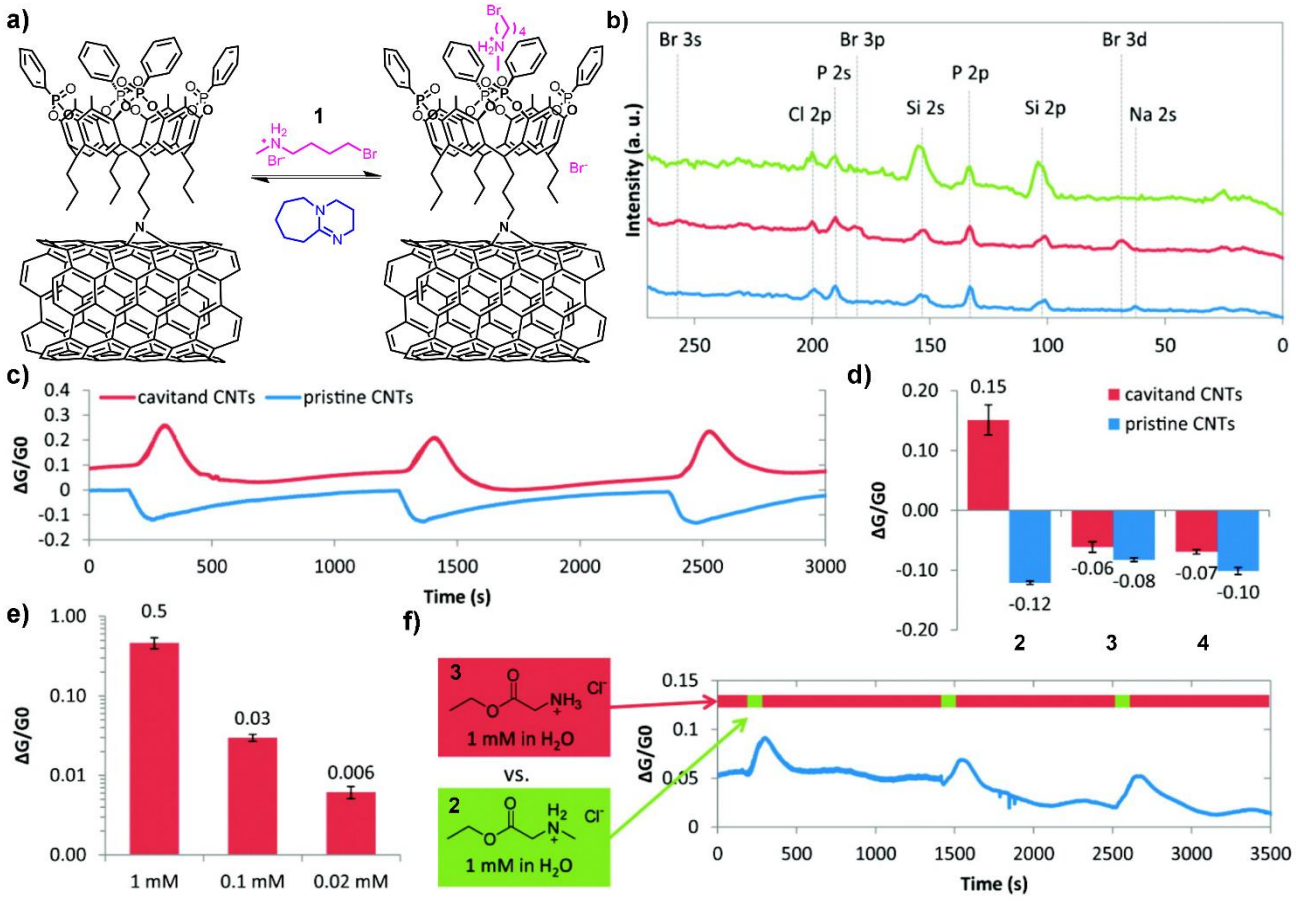

Figure 8. a) Reversible binding of 4-bromo-N-methylbutylammonium bromide guest **1**; b) XPS analysis of Tiiii•SWCNTs before exposure to **1** (blue), after exposure to **1** (red), and after subsequent washing with DBU (green). Si signals are due to the utilized Si substrate; c) Tiiii•SWCNTs and pristine SWCNTs show opposite responses upon exposure to a 1 mM solution of **2**; d) comparison of the current change upon exposure of Tiiii•SWCNT and pristine SWCNT devices to guests **2**-**4**; error bars are based on three consecutive measurements. e) response of Tiiii•SWCNT devices to different concentrations of **2**; error bars are based on three consecutive measurements. d) Response of Tiiii•SWCNT devices to alternating exposure to **2** and **3**. All the measurements were performed at pH 5, below the sarcosine pKa. Adapted from reference 57.

To overcome these problems, electrochemiluminescence (ECL)[62] was employed as transduction mode. ECL allows to obtain sensors with very low background and high sensitivity, good temporal and spatial resolution, robustness, versatility, and low fabrication costs. In ECL applications, the most used labels/co-reactant couple is a polypyridine ruthenium complex, like $Ru(bpy)_3^{2+}$ (Figure 9a), coupled with an amine. In this case sarcosine was used as co-reactant, since this secondary amine possesses sufficient energy requirements for generating the excited state of the fluorophore (Figure 9b). The tetraphosphonate cavitand, equipped with an azide group at the lower rim, was covalently attached onto magnetic microbeads (MMBs), functionalized with propargylamine units, *via* click chemistry. The resulting Tiiii•MMB sensor was tested for the selective capture of sarcosine hydrochloride in urine.[63] The analytical protocol consisted of three main steps, as reported in Figure 9c: (1) Capturing: at pH 5 the protonated form of sarcosine is efficiently complexed by Tiiii•MMB; (2) Separation: the beads are captured and separated from the matrix by means of a magnetic field, extracting selectively the sarcosine hydrochloride@Tiiii complex from urine; (3) Release and Detection: sarcosine is released as free base by increasing the pH to 12, above the sarcosine pKa. Luminophore **5** was then added, and the resulting solution deposited on disposable screen-printed electrode for ECL generation.

The calculated LOD and LOQ were 30 µM and 50 µM, respectively. The developed sensor resulted suitable for sarcosine detection in urine in the µM-mM window, a concentration range that encompasses the diagnostic urinary value of sarcosine in healthy subjects and PCa patients, respectively. In particular, these results indicate that this ECL-supramolecular approach is extremely promising for the detection of sarcosine and for early stage prostate cancer diagnosis and monitoring.

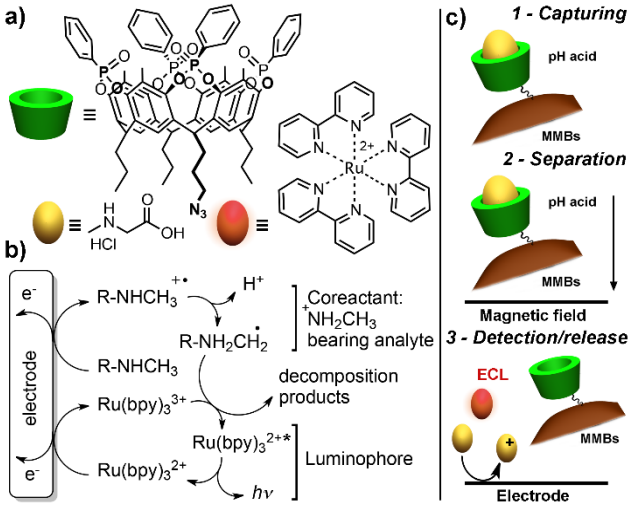

Figure 9. a) Structure of azide-functionalised tetraphosphonate cavitand, sarcosine hydrochloride and $Ru(bpy)_3^{2+}$; b) Schematic representation of ECL co-reactant "oxidative-reduction" mechanism; c) Schematic representation of the three steps protocol analysis. Adapted from reference 63.

4.2 Sensing of lysine post-translational protein modifications with cavitands

Post-translational modifications in proteins have a large influence on gene expression.[64] Histones have cationic amino-terminal tails ($-NH_3^+$) that are subjected to several PTMs, such as the mono, di and tri-methylation of the ε-amine of lysines.

In 2016, Hooley, Zhong and collaborators presented a fluorescence displacement sensing system for the detection of trimethylated lysine peptides and determination of histone demethylase activity based on a self-aggregating, water soluble deep cavitand (Figure 10).[65] This versatile receptor is capable to selectively recognize a wide variety of substrates in aqueous,[66] membranes and living cell environments.[67] The combination of tetracarboxylate cavitand (**1,** Figure 10a) and a suitable fluorophore allows sensing of KMe3 peptides *via* fluorescence displacement assay (FDA). The selected fluorescent guests were fluorescine-based dyes functionalized with ethylenediamine derivatives bearing, one, two or three methyl groups. Di and mono-methylated $NHMe_2^+$ dye **5**, NH_2Me^+ dye **6** and fluorescein have increasingly smaller affinities for **1**, due to mismatches in shape and charge-fitting with the cavity of host **1**. Their binding is sufficiently robust to be retained in a non-homogeneous environment, but at the same time sufficiently weak to be displaced by the NMe_3^+ dye **4**. For the **1•4** complex the dissociation constants K_d was estimated to be 17 ± 10 µM, while for the complexes between **1** and guests **5**, **6**, and fluorescein the K_d values were at least 10 times larger, indicating weak or nonspecific binding. Guest **4** showed a unique aggregation-based quenching mechanism, clearly different from the standard indicator displacement assays that occur exclusively *via* host-guest quenching interactions. This fluorescence decrease is ascribed to aggregation of the **1•4** complex, in which the fluorescein groups are close to one another. This phenomenon was exploited to establish a simple, in-solution displacement assays for the detection of trimethylated lysines, sufficiently strong to displace dye **4**. PTMs were selected as first target, focusing the attention on variably methylated H3 peptide fragments at the lysine 9 position (from zero to three methyl groups: H3K9, H3K9Me, and H3K9Me3). These fragments were titrated into a PBS solution of preformed **1•4** complex, and only the addition of the trimethylated peptide H3K9Me3 caused a significant recovery of the fluorescence signal. In the presence of pristine H3K9 at concentration above 5 µM, the observed fluorescence decreased significantly. The Authors demonstrated that the quenching was due to aggregation mediated by the electrostatic interaction between the cationic histone peptide and the anionic **1•4** complex, being controlled by the presence of chaotropic anions in solution. This electrostatically induced aggregation at high peptide concentration was not significant with H3K9Me3. This behaviour is presumably due to the suppression of H-bonding by the replacement of hard NH_3^+ ions with the softer NMe_3^+. This leads to a large signal difference between the unmethylated and trimethylated peptides, allowing a second level of discrimination between hard NH_3^+ and soft NMe_3^+ cations. This allows to test the monitoring of the histone demethylation processes in solution. To this aim, histone demethylase JMJD2E, which catalyses the demethylation of histone H3 at lysine residue 9, was employed. The addition of 100 nM JMJD2E and its cofactors to a buffered solution containing H3K9Me3 linked to **1** and free **4** initiated the demethylation reaction. The observed fluorescence signal continuously decreased over time, since the demethylated products H3K9Me2 or H3K9Me have much lower affinity for the cavitand and cannot compete with **4**. When no more demethylated product was generated, a plateau was reached. In this way a useful protocol for the lysine methylation PTM of proteins was developed in solution, which was then applied for a real sensor array.[68] Three different deep cavitands, featuring respectively carboxylates (**1**), hydrogens (**2**) and ammonium (**3**) substituents at the upper rim were inserted together with the reporting fluorescent guest **7** in a 96-well plate to produce an arrayed supramolecular tandem assay (Figure 10c). The wells were exposed to a mixture of three H3 peptides trimethylated at different lysine positions (H3K4Me3, H3K9Me3, H3K27Me3) to test the ability of the array perform site-selective KMe3 recognition. The fluorescence recovery of each well upon exposure to the peptide mixture were recorded and the readouts analysed *via* principal component analysis (PCA).

Journal Name

ARTICLE

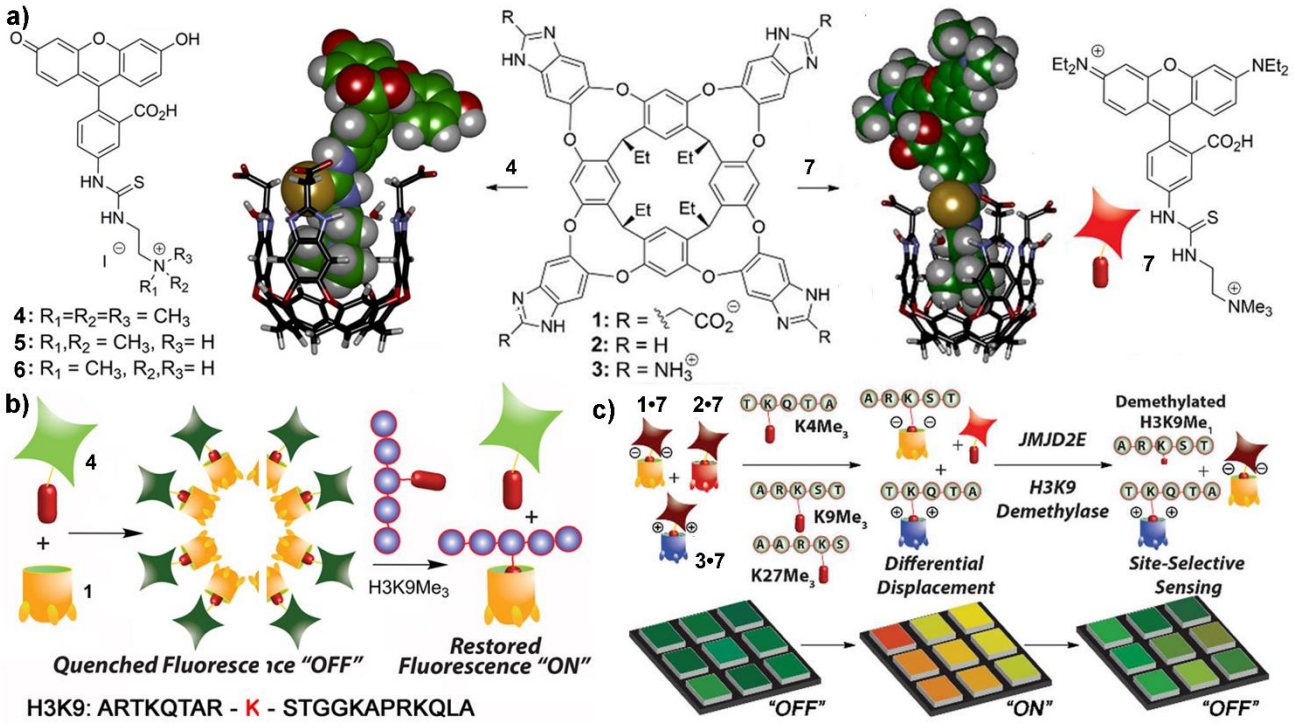

Figure 10. a) Structure of hosts **1–3**, guests **4-7** and a minimized model of the **1·4** and **1·7** host-guest complexes (SPARTAN); b) Aggregation-based sensing system; c) Supramolecular tandem assay for a lysine demethylase enzyme. Adapted from references 65 and 68.

The selectivity was tested by switching a single KMe3 peptide from the mixture with its non-methylated control. The sensor array was able to detect the absence of each methylated lysine in the peptide mixture, as well as different proportion of each KMe3 peptide *versus* the corresponding non-methylated peptide, proving that the array is able to monitor the progression of an enzymatic reaction. The robustness of the sensor was positively checked analysing a complex peptide mixture prepared by digesting bovine histones at a concentration of 5−250-fold of the H3K9Me3 peptide. It proved to be tolerant to the presence of chemicals and cofactors required for JMJD2E catalysed demethylation. As additional bonus, the cavitand inclusion protects guest **7** from photobleaching.

The ability of the array to monitor the enzyme activity of two different histone methylation agents was tested as well. The Authors focused the attention on lysine demethylase JMJD2E and the lysine methyltransferase PRDM9, which catalyses the tri-methylation of H3 at lysine residue 4. As the demethylation reaction proceeds, the displacement of the guest **7** from cavitand **1** decreased, thus lowering fluorescence emission. The opposite was observed when the activity of PRDM9 was monitored upon K4Me3 formation. Having separately shown the ability of the sensor in enzyme monitoring and site-selective KMe3 sensing, the Authors moved on to sense a specific peptide substrate for the methylation enzyme from a mixture of peptide with the three-component array. For the JMJD2E-catalyzed demethylation reaction, the analyses demonstrated that the sensor was able not only of distinguishing incorrect reaction products, but also the state of the product: fully demethylated K9 is distinguishable from K9Me1. For the PRDM9-catalyzed methylation reaction, the results showed that the reaction mixture contained only K4Me3 product with no trace of products with K9 or K27 methylation. Overall, the combined use of three cavitands in a fluorescence displacement array makes possible to recognize specific peptide modifications from a mixture of peptides in real enzymatic reactions.

However these cavitands are effective only for trimethylated lysine residues present in proteins. The related mono-methylation of lysine is an even more challenging modification to identify and measure with common direct physicochemical methods. Moreover, antibodies with little or no dependence on the local amino-acid sequence are difficult to develop.[64a] The specificity demonstrated by tetraphosphonate cavitands (Tiiii) in detecting *N*-mono-methylated lysine in water and PBS solutions,[55] inspired Dalcanale and co-workers to transfer this ability in detecting lysine mono-methylation in human histone H3 tails.[69] The synergic role played by cation–π interactions[45] of the acidic $^{+}NH_2$–CH_3 group with the π-basic cavity together

with steric complementary favours the complexation of mono-methylated ammonium salt respect to pristine, di- and tri-methylated ammonium anions.[51] Non-plasmonic Surface Enhanced Raman Scattering (SERS) was selected for the signal transduction coupling Tiiii receptors to all-dielectric resonators made of SiO_2/TiO_2 core/shell (T-rex) colloids.[70] They analysed a library of five peptides, referred as PC, P1, P2, P3 and P123, consisting of a sequence of 15 amino acids N-terminated with a 9-fluorenylmethyloxycarbonyl (FMOC) moiety as labelling agent. Three lysine residues are present on each peptide in position 4, 9 and 14 (Lys4, Lys9, and Lys14). Peptide PC, which presented no methylated lysine residues, was used as negative control. Peptides P1, P2 and P3 bore one mono-methylated lysine residue in position 4, 9 and 14, respectively. Finally, peptide P123 displayed all the three lysine residues mono-methylated (Figure 11). The peptides are first captured in solution by Tiiii that selectively binds their Lys-NMe^+ moieties. Separation from solution and detection of the peptide-Tiiii complexes is then enabled in one step by the T-rex core–shell resonator, which captures the complex and operates fully reproducible signal transduction by non-plasmonic SERS. To this purpose the cavitand must be equipped with a carboxylic group at the lower rim for grafting on the TiO_2 surface. The complexation driven chemisorption of the peptides on the T-rex surface is dependent on the number of mono-methylated lysines present in the H3 histone tail. P123 is retained stronger than the other monomethylated histones on the surface thanks to the multiple binding mode.

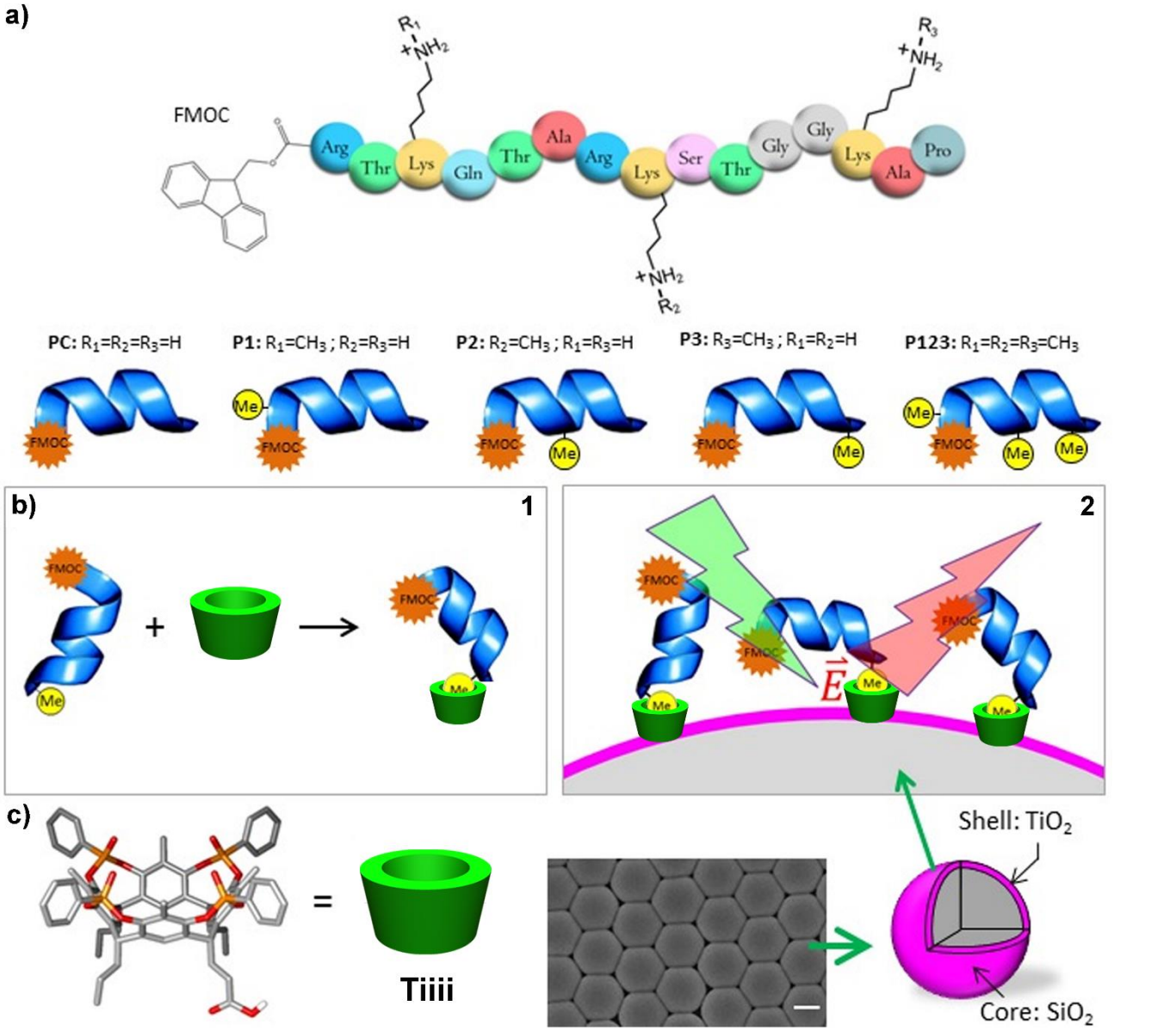

Figure 11. Materials (a, c) and experimental (b) design for recognition–separation–probing of lysine mono-methylated histone H3 tail peptides by a supramolecular recognition and T-rex non-plasmonic SERS. For a detailed description refer to the main text. In the SEM image in the bottom left panel the scale bar is 1 µm. Adapted from reference 69.

Journal Name

ARTICLE

The selectivity of Tiiii receptors in binding methylated lysine residues forming stable complexes was then challenged in solutions containing both trimethylated (P123) and non-methylated (PC) peptides, which is relevant in view of applications in common protein extracts. P123 is fully retained while PC is not.

4.3 Choline detection with octaamide cavitands

Choline and its derivatives, like acetyl choline, carnitine and choline phospholipids are linked to many important biological processes. In particular, choline is an essential nutrient,[71] acetyl choline is an important excitatory neurotransmitter,[72] carnitine is involved in the metabolism of lipids,[73] and choline-containing phospholipids are responsible for important properties of the cell wall.[74] The well-established methodologies for choline detection,[75] mainly based on radio-enzymatic and chemiluminescent assays,[76] liquid chromatography[77] and amperometric techniques[78] suffer of several drawbacks, mostly related to the sample pre-processing steps to extract and pre-concentrate the target analytes. To overcome these disadvantages Ballester and Rius presented a new solid-contact ion-selective electrode to determine choline and derivatives in aqueous solutions based on the molecular recognition abilities of octaamide cavitand **1** in the hydrophobic environment of the polymeric membrane (Figure 12a).[79] This cavitand is known to bind trimethyl alkyl ammonium cations such as choline, acetylcholine or carnitine.[80] A potentiometric sensor was built, covering a SWCNT electrode with an acrylic matrix layer containing the cavitand as ionophore. The SWCNT electrode converts the ionic current in the polymeric membrane into the electronic current that flows through a glassy carbon as electronic conducting substrate (Figure 12b). As lipophilic anion tetrakis(4-chlorophenyl)borate was used, to allow the primary choline cation to be distributed between the two immiscible water/organic phases.[81] The developed sensor was tested by electrochemical impedance spectroscopy to observe the behaviour of the membrane in the electrode, and characterized by environmental scanning electron microscopy to measure the membrane thickness. The new electrode displayed very stable behaviour throughout the dynamic range (10^{-5} to 10^{-1} M) used in the study. The calibration curves for choline were determined by consecutive additions of different concentrations and the limit of detection (LOD) was determined to be $10^{-6.4}$ M. The potentiometric selectivity coefficients of the sensor was tested against major interferents present in the blood, namely acetyl choline, acetyl-l-carnitine, carnitine, trimethylamine, glucosamine, l-alanine, ammonium and sodium (Figure 12a). In particular, acetyl choline was chosen to demonstrate the compatibility of the cavitand towards choline and derivatives, while acetyl-l-carnitine, trimethylamine, alanine and glucosamine were selected to evaluate the influence of hydrophilicity towards selectivity. The last two analytes, ammonium and sodium, were selected to evaluate the selectivity of the ionophore towards small ions. The observed selectivity is determined by the interplay between two parameters: the ion-exchange ability of the polymeric membrane and the molecular recognition properties of the entrapped cavitand. Choline and acetylcholine are slightly preferred analytes over acetyl-l-carnitine and trimethylamine because of their higher hydrophobicity, despite having the same trimethylammonium binding group. In the case of ammonium and sodium the lack of CH-π interactions and the high energy required for

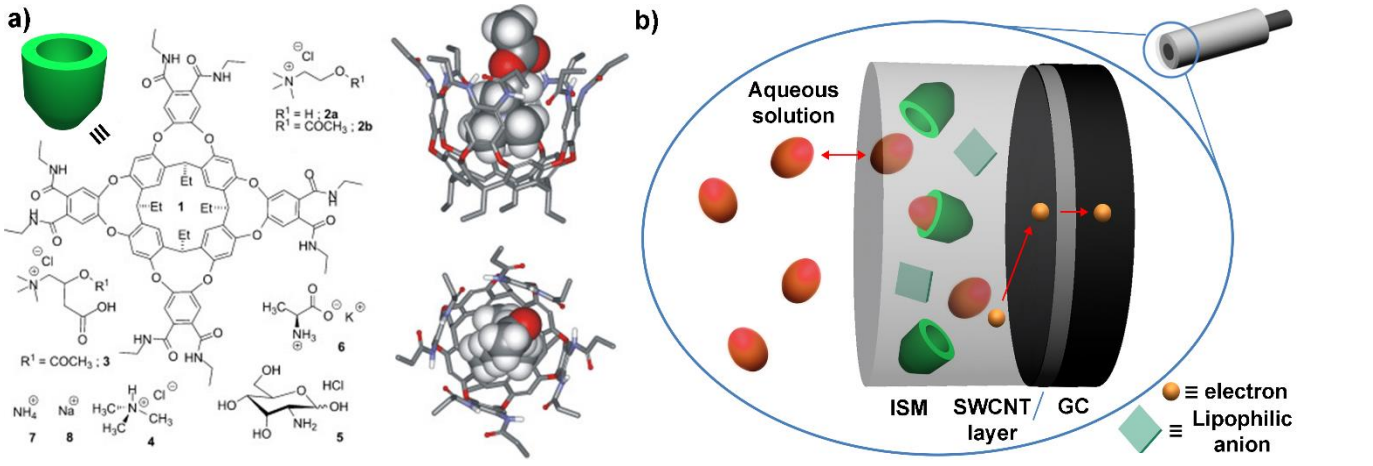

Figure 12. a) Molecular structures of the octaamide cavitand **1** and the ions tested in this study (**2a**: choline, **2b**: acetylcholine, **3**: carnitine, **4**: trimethylamine, **5**: glucosamine, **6**: l-alanine, **7**: ammonium, **8**: sodium). Side and top views of the octaamide cavitand–acetylcholine complex. **b)** Schematic representation of the various parts of the solid-contact ion-selective electrode developed. The zoom shows the representation of the transduction process (ion-to-electron) due to the intrinsic large capacitance of the interface SWCNT-membrane. Adapted from reference 79.

Journal Name

ARTICLE

desolvation, hinder the interaction between these cations and the cavitand. The present potentiometric sensor, despite of its reduced selectivity, shows an original way to transform a molecular recognition event in a potentiometric signal. The host-guest interaction takes place in the acrylate ion-selective membrane of the solid-contact electrode, creating an ionic current that is converted by the SWCNT into electronic current.

4.4 Methamphetamine sensing with tetraphosphonate cavitands

A specific sensor for methamphetamines and related designer drugs[52] has been developed by grafting tetraphosphonate cavitands on silicon microcantilevers (Si-MC, Figure 13a).[82] The surface molecular recognition is translated by MCs into nanomechanical work with high fidelity, reproducibility, and robustness. In particular, MC nanomechanical transduction is "energy-based" and occurs regardless the analyte mass in a label-free fashion. The free energy released by a host-guest interaction confined at a solid-solution interface splits into chemical and mechanical surface work, the latter determined by the work that the host performs to accommodate the guest.[83] This work derives from a variation of the surface stress (surface pressure) that the MC balances by bending. The stronger the interaction the larger the bending.

In detail, a Tiiii cavitand bearing ω-decylenic feet was covalently grafted on the H-terminated Si(100) face of Si-MC by photochemical hydrosilylation of the double bonds. The developed Tiiii-Si-MC sensor resulted efficient in detecting the whole class of methamphetamine in water, irrespective of the substituent attached to the $^{+}NH_2$-CH_3 group. The developed sensor was the first example of a device capable to single out the entire methamphetamine class and to recognize the so called "designer drugs", that are the result of minor modifications in the chemical structure of an existing drug, but showing pharmacological effects similar to its archetype. Analogues of amphetamine and methamphetamine are among the most commonly known types of designer drugs and pose serious challenges to the current lab- and on-site-detection technologies, normally optimized for identification of a specific drug or substance rather than for the recognition of the entire drug family. The interaction modes responsible for the drug complexation by Tiiii were disclosed by the molecular structures of the corresponding complexes in the solid state, obtained by X-ray diffraction analysis on single crystals and reported in Figure 13b-d. In all the structures, two strong hydrogen bonds between the ammonium $^{+}$N-H and the P=O of the cavitand are present.

Further stabilization is given by cation–π and CH-π interactions between the aromatic cavity of the host and the available methyl groups of the drugs. MDMA, known as ecstasy and 3-FMA (related designer drug) interact with the cavitand exactly in the same way despite their different aromatic substituents

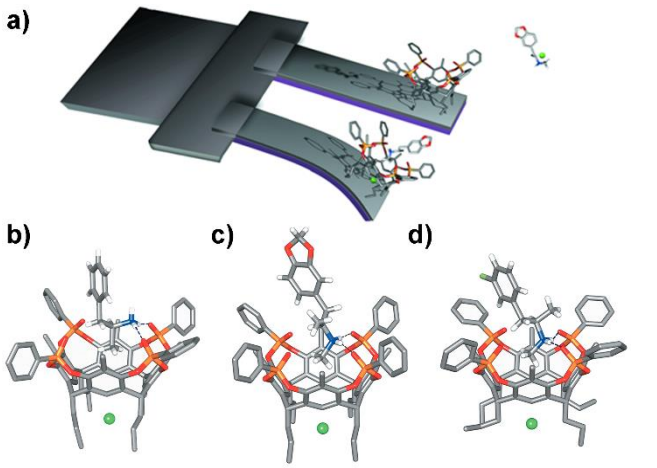

Figure 13. a) Schematic representation of guest recognition induced microcantilever deflection; molecular structures of the complexes b) Tiiii·amphetamine, c) Tiiii·MDMA, and d) Tiiii·3-FMA hydrochlorides. C gray, O red, P orange, N blue, Cl and F green, H white, H-bonds blue dotted lines. For clarity, the H atoms of the Tiiii have been omitted. Adapted from reference 52.

(Figure 13 b and c). In these two cases the methyl group draws its parent nitrogen atom deeper inside the cavity, thus enhancing the strength of charge–dipole interactions.

An array of four functionalized MCs was exposed to a 1 x 10^{-4} M water solution of MDMA, amphetamine, and caffeine, which is a known excipient. In the case of drugs, a deflection of the MCs was detected due to the interaction between the hosts and the grafted Tiiii, while for caffeine no significant deflection was observed, despite the presence of three potentially interacting *N*-methyl groups in the molecule. The nominal detection limit of the developed Tiiii-Si-MC array for ammine-based drugs in water was calculated to tenths of ppm, one order of magnitude lower than the reported LOD for molecular imprinted polymer (MIP) coated QCM.[84] The sensor was also tested on a real "street" sample containing FMA and glucose, a common excipient used in drug formulations. All the experimental results were supported performing control experiments using a Si-MC decorated with a parent cavitand which is ineffective in complexing methyl ammonium salts.

5. Cucurbit[*n*]urils

Cucurbit[*n*]urils (*n* = 5-8 and 10; CB[*n*]) are water soluble cyclic methylene-bridged glycouril oligomers.[85] These molecular receptors are barrel-like macrocycles with two identical portal regions laced by ureido-carbonyl oxygen atoms. The number of glycouril groups determines the size of the CB[*n*] cavity without affecting the height (approximately 0.9 nm). CB[*5*] and CB[*7*] are quite soluble in water, while CB[*6*] and CB[*8*] are poorly soluble in aqueous environment. The solubility of all cucurbiturils in common organic solvents is less than 10^{-5} M,

Journal Name

ARTICLE

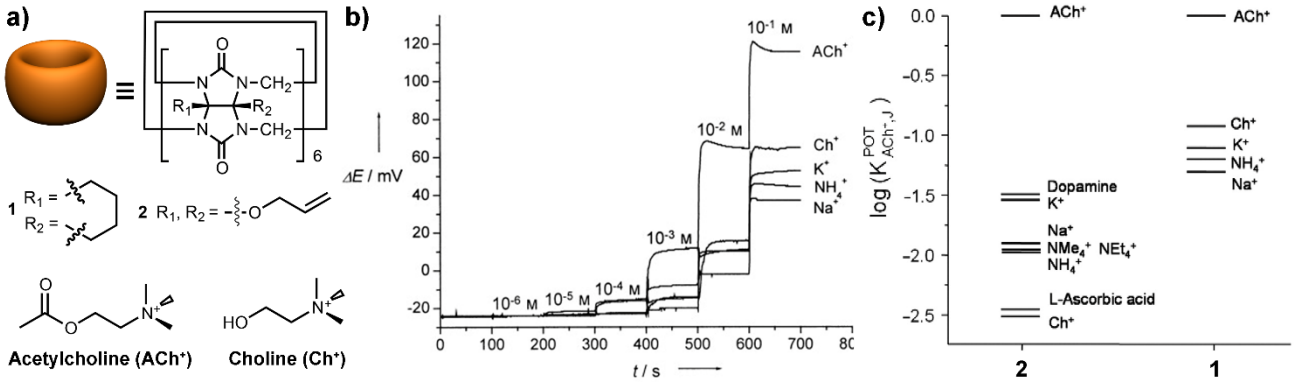

Figure 14. a) Chemical structures of ACh⁺, Ch⁺ cyclohexane-functionalized CB[*6*] (**1**), (allyloxy)$_{12}$CB[*6*] (**2**); b) Responses of an ISE based on **1** to ACh⁺ and other interfering ions, used as chloride, including Ch+ (pH 7.2 with 10 mM 2-amino-2-(hydroxymethyl)-1,3-propanediol (Tris) buffer); c) Comparison of selectivity coefficients of two CB[6]- based ISEs. Adapted from references 96 and 97.

limiting their use to aqueous media. Multiple intermolecular interactions are involved in guest complexation by CB[*n*], such as non-classical hydrophobic effect, due to the release of "high-energy water" upon inclusion of non-polar organic residues,[86] ion-dipole interactions and hydrogen bonding involving the two ureido carbonyl rims.

CB[*n*] host–guest chemistry found the majority of its analytical applications in the detection of biologically relevant analytes or ions in water, involving spectroscopic techniques.[87] In this field, except for few examples of CB[*n*] derivatization with chromophoric groups,[88,89] the non-chromophoric nature of pristine CB[*n*] limits their sensing applications to dye displacement assays relying on competitive processes.

5.1 Electrochemical sensing with cucurbiturils

The first electrochemical sensor based on a cucurbit[*n*]uril modified electrode was reported by Quintanta and co-workers in 2011.[90] The Authors proposed the use of a CB[*8*] glassy carbon modified electrode for tryptophan (Trp) electrochemical determination. This amino acid is a precursor of relevant biomolecules, such as serotonin, and its improper metabolism has been listed as a possible cause of schizophrenia. Preliminary electrochemical experiments in solution revealed that Trp inclusion in CB[*8*] cavity, previously observed by Urbach et al.,[91,92] generates the highest E_p shift (ca. 100 mV) for the Trp response to more positive values and a decrease in the oxidation current. The glassy carbon electrode was modified by immersion in an homogeneous ethanol suspension of CB[*8*] (0.35% w/v) and Nafion (0.25% w/v), a perfluorinated sulfonated cation-exchange polymer with excellent antifouling capacity, chemical inertness and high permeability to cations. After optimization of all the parameters related both to the electrode modification and the differential pulse Trp response, detection and quantification limits in 0.5 M H_3PO_4 solutions at pH 2.2 were found to be 1.43 × 10^{-7} M and 4.36 × 10^{-7} M, respectively. Accuracy and precision of the proposed method have been evaluated, as well as inter-day reproducibility, proving the robustness of the experimental design. To evaluate the selectivity of the proposed method, Trp response was measured in the presence of different amino acids and other possible interferents, such as acetylcholine (AcCh), ascorbic and uric acid. The tested substances significantly altered the Trp peak current, with tyrosine being the major interferent, with an oxidation wave at a potential very close to the Trp one. The applicability of CB[*8*] modified electrode to the detection of Trp in human serum was finally evaluated. No matrix interference was reported, together with a relative standard deviation (RSD) value lower than 0.62% (n=3), thus confirming that this method can be applied with sufficient precision to Trp analysis in real samples.

CB[*8*] was also exploited for the development of an electrochemical sensors for dopamine.[93] PVC and Nafion were used as matrixes to incorporate CB[8] onto the glassy carbon electrode surface with no loss of reproducibility under flow conditions over time. This method achieved dopamine detection limits in the nanomolar range, even in the presence of ascorbic acid as interferent.

Also the smaller CB[*7*] was employed to impart selectivity to electrochemical sensors. Enzyme-catalysed digestion and release of electroactive methylene blue coupled with CB[*7*] derivatized electrodes have been applied to the detection of different proteins[94] and matrix metalloproteinase-2.[95]

5.2 Amperometric detection of acetylcholine using CB[*6*]

Acetylcholine (ACh⁺) is a prominent neurotransmitter in the human central nervous system, and a deficiency in ACh⁺ is associated with various neurodegenerative diseases, including Alzheimer's. Common detection methods involve amperometric sensors based on acetylcholine esterase (AChE) enzyme immobilization. Such methods reach detection limit

Journal Name

ARTICLE

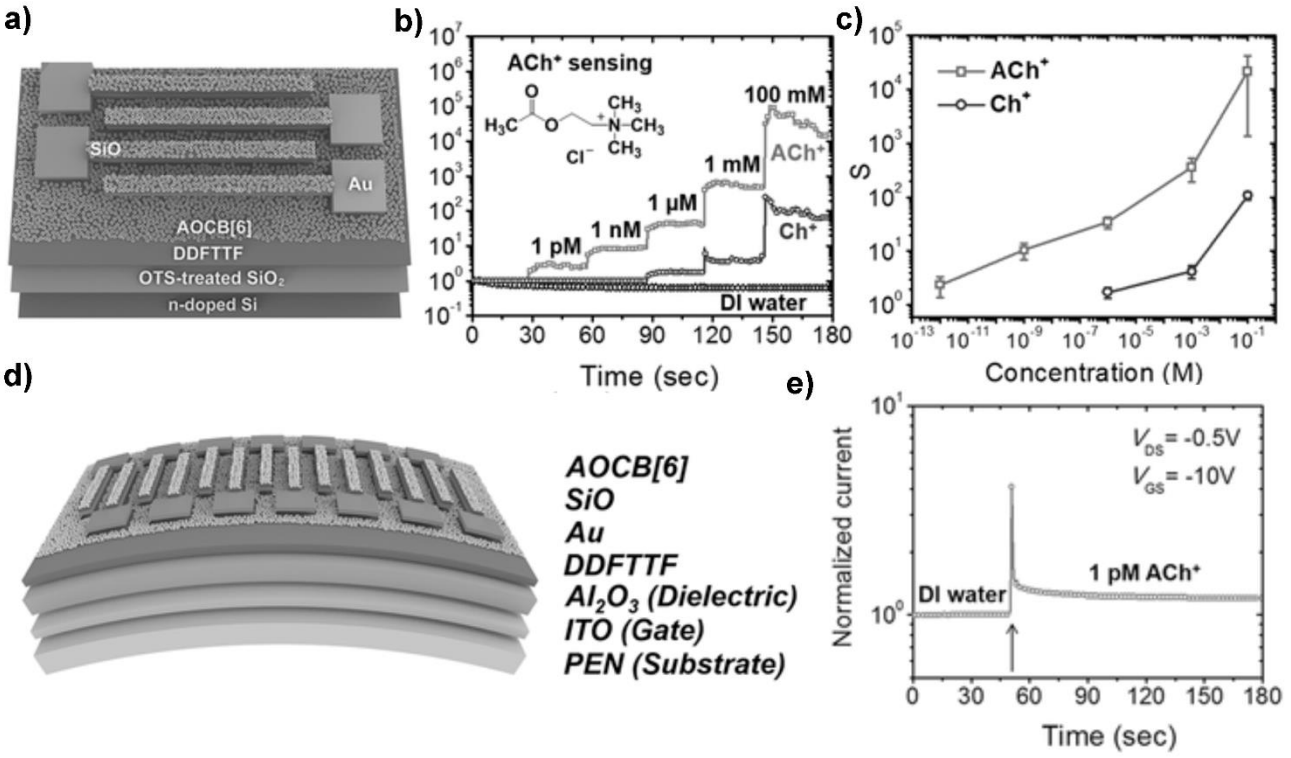

Figure 15. a) Schematic illustration of the top-contact OFET-based sensors with a synthetic receptor **2**; b) Real-time responses of DDFTTF OFET-based sensors with **2** toward various concentrations (from 1×10^{-12} M to 0.1 M) of ACh^+ and Ch^+, and pure deionized water; c) Statistical comparisons of the sensing results for ACh^+ and Ch^+ (*S* indicates $I_D/I_{D\text{-}BASE}$); d) Schematic illustration of flexible DDFTTF OFET-based sensors with **2**; e) Real-time responses of the sensors with **2** toward 1×10^{-12} M ACh^+ under a low-voltage operating condition. Adapted from reference 98.

down to the sub-nM range, but suffer for shortcomings such as high cost, lack of long-term stability, and complicated fabrication processes. As a reliable alternative, Kim and co-workers proposed low-cost and high-performance electronic ACh^+ sensors based on ion-selective electrodes (ISEs) functionalized with CB[*6*] derivatives. [96] The ability of the CB[*6*] **1** bearing six equator-bound fused cyclohexane units (**1**, Figure 14a) to differentiate acetylcholine from choline was demonstrated in neutral water. Its good solubility in organic solvents allowed the preparation of membrane electrodes for ACh^+ detection by slow evaporation of a solution of 1 wt% of **1** in MeOH, 33 wt% PVC and 66 wt% dioctyl adipate (DOA) in THF, as plasticizer. The prepared ISEs show high selectivity for ACh^+ over choline (Ch^+) and other interfering ions such as Na^+, K^+, and NH_4^+ (Figure 14b).

Similarly, an ISE for ACh^+ detection was prepared using $(allyloxy)_{12}$CB[*6*] (**2**, Figure 14a).[97] This membrane electrode showed excellent performance in detecting ACh^+, with a linear response down to ca. 10^{-6} mol dm^{-3}, and high selectivity over Ch^+ (log K^{POT} = -2:5, Figure 14c). The comparison of the selectivity coefficients of two electrodes, reported in Figure 14c, shows that **2**-based ISE presents an higher selectivity for ACh^+ over Ch^+ and other interfering ions. Considering that the sizes and shapes of the two cavities are essentially the same, this increment arises from the different lipophilicity of the two CB[*6*] derivatives, that affects the miscibility of the ionophore within the plasticised PVC membrane and therefore the ISE performances.

Since the achieved detection limits in the µM range for ACh^+ are insufficient for early-stage disease diagnosis, more recently Kim and co-workers turned to organic field-effect transistor (OFET)-based transducers.[98] OFET-type devices amplify electrical signals obtained from binding events by tuning the applied gate voltage, leading to higher sensitivity compared to conventional sensors with two electrodes.[99] However, pristine OFET-based sensors often exhibit low selectivity for target analytes since all the components of the solution are capable of diffusing into the channel region through grain boundaries, affecting the detected signal.

For the detection of ACh^+, two different OFET-based sensors bearing **2** as selective sensing layer were prepared with bottom-gate top-contact configuration. In both cases, by virtue of its relatively high mobility and operational stability in water, the *p*-channel semiconductor 5,5′-bis-(7-dodecyl-9H- fluoren-2-yl)-2,2′-bithiophene (DDFTTF) layer was chosen as the active layer.[100] In the first set-up (Figure 15a), the DDFTTF thin film

was thermally evaporated onto *n*-octadecyltrimethoxysilane (OTS)-treated SiO_2/Si. Source and drain electrodes were obtained by gold evaporation through a shadow mask and then passivated with a SiO layer to prevent their peeling off during the OFET sensor operation in water. The semiconductor was functionalized *via* spin-coating with a homogeneous layer of CB[*6*] derivative **2**, which is soluble in methanol but insoluble in water. The so obtained OFET-based sensor exhibited a positive sensing behaviour, since the drain current was enhanced after injection of the analytes, with a detection limit down to 1×10^{-12} M of ACh^+. This measured value is six orders of magnitude lower than that of the best performing ISE-based sensors described above, and two orders of magnitude lower than that of AChE-based biosensors (1×10^{-10} M).[101] The OFET-based sensor also allowed the selective discrimination of ACh^+ over common interferents such as Ch^+ and sodium ion, since no signals for these interferents were detected at μM concentrations (Figure 15b, Figure 15c). In PBS solution (pH 7.4, 0.01 M) the device sensitivity was lower compared to deionized water due to the ionic strength of the medium.

Similar results in terms of sensitivity and selectivity were obtained under low-voltage operation conditions (Figure 15e) with a flexible OFET design (Figure 15d): a 100 nm thick aluminium oxide (Al_2O_3) gate transparent dielectric layer was deposited on indium tin oxide (ITO)-coated polyethylene naphthalate (PEN) via a radio frequency (RF) magnetron sputtering technique.[98]

Among cucurbiturils, CB[7] has been shown to be the most versatile, able to encapsulate drugs of abuse into its cavity, as shown by the crystal structure of CB[7]·methamphetamine.[102] As for sensing, a cross-reactive array for the detection of opiates in water and urine has been proposed, using three acyclic cucurbiturils.[103] The recognition event between these open CBs and guests like heroin results in modification of the fluorescence of the terminal walls, according to the relative affinity of each analyte with the receptors.

6. Pillar[*n*]enes and molecular tweezers

Pillar[*n*]enes (or pillararenes, n=5-10) are a relatively new class of supramolecular receptors which were firstly synthesized in 2008 by Nakamoto and *co*-workers.[104] These synthetic macrocyclic host compounds are composed of hydroquinone units linked by methylene bridges at *para*-positions. Pillar[*n*]enes present pillar-shaped, very rigid and π-rich cavities with peculiar host–guest properties. They have alkoxy groups at both cavity rims, that make them good building blocks for molecular recognition applications.[105] The binding affinities and abilities of pillarenes for specially designed guests can be tuned by changing the internal cavity dimensions, namely increasing or decreasing the number of the hydroquinone units or substituting the alkoxy groups with specific functional groups, in order to increase the number of host-guest interactions involved in the complexation.[105] These new functionalities can also be used to impart solubility in water.

In 2017, two reviews were published summarizing the use of these macrocycles in biological and related applications, like in drug delivery[106] and biomedical imaging.[107] Their use in biosensing has been limited to the detection of lysine and arginine in water via indicator displacement assay.[108] So far pillarenes have not been coupled with suitable transducers for the generation of real sensing devices. However their remarkable complexation properties toward biologically relevant analytes are partially orthogonal with respect to those of the macrocyclic receptors discussed above, making them very appealing candidates for abiotic sensing.

Molecular tweezers are noncyclic host molecules presenting torus-shaped cavities surrounded by convergent aromatic rings.[109] The pioneering work of the Schrader group has shown their unique ability to bind lysine and arginine residues in proteins with strong affinity, once made water soluble.[110] The protein camouflage with molecular tweezers leads to inhibition of enzymatic activity and modulation of protein assembly, with promising therapeutic perspective for treatment of Alzheimer's and Parkinson's diseases.[111] These outstanding molecular recognition properties toward biomolecules has not been turned into a sensing device so far.

7. Conclusions and outlook

Biochemical sensing is one of the most challenging endeavours in sensor technology. The concurrent requirements of specificity in analyte detection and high sensitivity, typically in the μM range, are exacerbated by the need to operate in complex matrices containing a large number of potential interferents. These requirements put under severe strain all possible solutions amenable to be used in preventive healthcare. Nevertheless, the social and economic needs of cheap and reliable screening technologies for diseases like cancer, diabetes, Alzheimer – just to mention the major ones – are so critical to impose this topic to the agenda of most major funding agencies and research institutions.

Since the number and type of the biological markers of interest is too wide to be covered by a single sensor technology, the use of macrocyclic receptors is gaining momentum as alternative to the most travelled immunological techniques in selected cases. The large pool of macrocyclic receptors available, their synthetic modularity, chemical purity and diverse complexation properties offer unparalleled opportunities for biochemical sensing. Macrocyclic receptors can be designed and prepared according to the analytical problem to be solved, thanks to the degree of sophistication reached in the fine tuning of weak interactions responsible of molecular recognition. Several transduction platforms are amenable to turn the molecular recognition events into a readable signal, provided that the receptors are integrated into solid state devices. As consequence, a large variety of sensors for preventive healthcare are potentially available by combining the pool of programmable receptors with the available transducer platforms.

According to these premises, the question is why do we still have so few sensors in healthcare.[6] As for biochemical sensors

based on macrocycles, the limited number of real sensor solutions present so far in the literature is due to two major hurdles. The technical one is the transfer of the intrinsic molecular recognition properties of a receptor at the water-solid interface and the high fidelity transduction of the interfacial molecular recognition events into a readable signal. The second is related to research compartmentalisation. This is a highly multidisciplinary field, where the practical success requires the concerted efforts of researchers having different backgrounds, namely chemists, engineers, biologists, medical doctors and even healthcare managers. Joining together all these competences is complicated and expensive, but necessary to move ahead the field and deliver the sensors technologies demanded by society. Only in this way the most promising molecular probes reported in the literature will move on from the proof-of-concept stage to become effective biochemical sensors.

Conflicts of interest

There are no conflicts to declare.

Acknowledgements

This work was supported by the European Union through the DIRAC project (FP7-SEC-2009-242309) and by Regione Lombardia-INSTM through the SNAF and SUPRANANO projects.

References

1 US National Cancer Institute's Surveillance Epidemiology and End Results (SEER).
2 M. Analoui, J. D. Bronzino and D. R. Peterson, *Medical Imaging: Principles and Practices*, CRC Press, Boca Raton, 2012.
3 P. J. Delves, S. J. Martin, D. R. Burton and I. M. Roitt, *Roitt's Essential Immunology*, John Wiley & Sons Chichester, 13th Edition, 2017.
4 T. A. Egelhofer, A. Minoda, S. Klugman, K. Lee, P. Kolasinska-Zwierz, A. A. Alekseyenko, M. S. Cheung, D. S. Day, S. Gadel, A. A. Gorchakov, T. T. Gu, P. V. Kharchenko, S. Kuan, I. Latorre, D. Linder-Basso, Y. Luu, Q. Ngo, M. Perry, A. Rechtsteiner, N. C. Riddle, Y. B. Schwartz, G. A. Shanower, A. Vielle, V. Ahringer, S. C. R. Elgin, M. I. Kuroda, V. Pirrotta, B. Ren, S. Strome, P. J. Park, G. H. Karpen, R. D. Hawkins and J. D. Lieb, *Nature Struct. Mol. Biol*, 2011, **18**, 91-94.
5 O. N. Jensen, *Nature Rev. Mol. Cell Biol.*, 2006, **7**, 391-403.
6 O. S. Wolfbeis, *Angew. Chem. Int. Ed.*, 2013, **52**, 9864-9865.
7 a) A. Fragoso, B. Sanromà, M. Ortiz and C. K. O'Sullivan, *Soft Matter*, 2009, **5**, 400-406. b) A. Fragoso, J. Caballero, E. Almirall, R. Villalonga and R. Cao, *Langmuir*, 2002, **18**, 5051-5054. c) X. Zhang, L. Wu, J. Zhou, X. Zhang and J. Chen, *J. Electroanal. Chem.*, 2015, **742**, 97-103. d) X. Shi, G. Chen, L. Yuan, Z. Tang, W. Liu, Q. Zhang, D. M. Haddleton and H. Chen, *Mater. Horiz.*, 2014, **1**, 540-545.
8 J. Lenik, *Curr. Med. Chem.*, 2017, **24**, 2359-2391.
9 E. Wajs, N. Fernández and A. Fragoso, *Analyst*, 2016, **141**, 3274-3279.
10 A. Harada, Y. Takashima and H. Yamaguchi, *Chem. Soc. Rev.*, 2009, **38**, 875-882.
11 A. Hashidzume and A. Harada, in *Multivalency: Concepts, Research and Applications*, ed. J. Huskens, L. J. Prins, R. Haag and B. J. Ravoo, John Wiley & Sons, 2018, 5, 123-138.
12 J. Jiang, X. Lin and G. Diao, *Appl. Mater. Interfaces*, 2017, **9**, 36688-36694.
13 W. Zhang, M. Chen and G. W. Diao, *Electrochim. Acta*, 2011, **56**, 5129-5136.
14 A. Alsbaiee, B. J. Smith, L. L. Xiao, Y. H. Ling, D. E. Helbling and W. R. Dichtel, *Nature*, 2015, **529**, 190-194.
15 a) T. Hou, W. Li, X. J. Liu and F. Li, *Anal. Chem.*, 2015, **87**, 11368-11374. b) S. Y. Li, R. Li, M. M. Dong, L. Y. Zhang, Y. Jiang, L. J. Chen, W. Qi and H. Wang, *Sens. Actuators B*, 2016, **222**, 198-204.
16 Z. Hua, Q. Qin, X. Bai, C. Wang and X. Huang, *Sens. Actuators B*, 2015, **220**, 1169–1177.
17 T. Feng, X. Qiao, H. Wang, Z. Sun, Y. Qi and C. Hong, *J. Mater. Chem. B,* 2016, **4**, 990-996
18 a) J. Mirenowicz and W. Schultz*, Nature* 1996, **379**, 449–451. b) J.M. Wilson, K.S. Kalasinsky, A.I. Levey, C. Bergeron, G. Reiber, R.M. Anthony,G.A. Schmunk, K. Shannak, J.W. Haycock and S.J. Kish*, Nat. Med.* 1996, **2**, 699–703.
19 a) S.S. Kumar, J. Mathiyarasu and K.L. Phani, *J. Electroanal. Chem.* 2005, **578**, 95–103. b) A. Imperato and G. Di Chiara, *J. Neurosci*. 1984, **4**, 966–977. c) J.B. Chien, R.A. Wallingford and A.G. Ewing, *J. Neurochem.* 1990, **54**, 633–638. c) H.Y. Wang, Y. Sun and B. Tang, *Talanta* 2002, **57**, 899–907.
20 R. Suresh, K. Giribabu, R. Manigandan, S.P. Kumar, S. Munusamy, S.Muthamizh, A. Stephen and V. Narayanan, *Sens. Actuators B* 2014, **202**,440–447.
21 a) S. Elhag, Z.H. Ibupoto, X. Liu, O. Nur and M. Willander, *Sens. Actuators B* 2014, **203**, 543–549. b) Y. Zhao, S.H. Li, J. Chu, Y.P. Chen, W.W. Li, H.Q. Yu, G. Liu, Y.C. Tian and Y. Xiong, *Biosens. Bioelectron.* 2012, **35**, 115–122. c) E. Molaakbari, A. Mostafavi and H. Beitollahi, *Sens.Actuators B* 2015, **208**, 195–203.
22 M. M. Rodríguez-Delgado, G. S. Alemán-Nava, J. M. Rodríguez-Delgado, G. Dieck-Assad, S. O. Martínez-Chapa, D. Barceló and R. Parra *Trends Anal. Chem.*, 2015, **74**, 21-45.
23 L. Mutihac, J. H. Lee, J. S. Kim and J. Vicens, *Chem. Soc. Rev.*, 2011, **40**, 2777–2796.
24 K. Ariga, H. Ito, J. P. Hill and H. Tsukube, *Chem. Soc. Rev.*, 2012, **41**, 5800–5835.
25 F. Perret, A. N. Lazar, and A. W. Coleman, *Chem. Commun.*, 2006, **23**, 2425-2438.
26 a) A. W. Coleman, F. Perret, A. Moussa, M. Dupin, Y. Guo and H. Perron, *Calix[n]arenes as Protein Sensors*, in *Creative Chemical Sensor Systems*, ed. T. Schrader, Springer-Verlag Berlin, Heidelberg, 2007. b) S. van Dun, C. Ottmann, L.-G. Milroy and L. Brunsveld, *J. Am. Chem. Soc.*, 2017, **139**, 13960-13968.
27 S. B. Nimsea and T. Kim, *Chem. Soc. Rev.*, 2013, **42**, 366-386.
28 D.-S. Guo and Y. Liu, *Acc. Chem. Res.*, 2014, **47**, 1925-1934.
29 S. A. Minaker, K. D. Daze, M. C. F. Ma and F. Hof, *J. Am. Chem. Soc.*, 2012, **134**, 11674-11680.
30 E. V. Anslyn, *J. Org. Chem.*, 2007, **72**, 687-699.
31 S. Stewart, M. Adams Ivy and E. V. Anslyn, *Chem. Soc. Rev.*, 2014, **43**, 70-84
32 R. Zadmard and T. Schrader, *J. Am. Chem. Soc.*, 2005, **127**, 904-915.
33 D. P. Nikolelis, S.-S. E. Petropoulou, E. Pergel and K. Toth, *Electroanal.*, 2002, **14**, 783-789.
34 D. P. Nikolelis, S.-S. E. Petropoulou and G. Theoharis, *Electroanal.*, 2003, **15**, 1616-1624.
35 J.-Y. Park, B.-C. Kim and S.-M. Park, *Anal. Chem.*, 2007, **79**, 1890-1896.
36 H-L Zhang, Y. Liu, G.-S. Lai, A.-M. Yu, Y.-M. Huanga and C.-M. Jinac, *Analyst*, 2009, **134**, 2141–2146.
37 G. A. Evtugyn, R. V. Shamagsumova, R. R. Sitdikov, I. I. Stoikov, I. S. Antipin, M. V. Ageeva and T. Hianik, *Electroanal*., 2011, **23**, 2281-2289.
38 X. Mao, H. Zhao, L. Luo, D. Tian and H. Li, *J. Mater. Chem. C*, 2015, **3**, 1325–1329.
39 P. A. Gale, P. Anzenbacher and J. L. Sessler, *Coord. Chem. Rev.*, 2001, **222**, 57-102.
40 T. Guinovart, D. Hernández-Alonso, L. Adriaenssens, P. Blondeau, M. Martínez-Belmonte, F. X. Rius, F. J. Andrade and P. Ballester, *Angew. Chem. Int. Ed.*, 2016, **55**, 2435-2440.
41 a) D. J. Cram, *Science*, 1983, **219**, 1177-1183. b) D. J. Cram and J. M. Cram, *Container Molecules and Their Guests*. Stoddart, J. F.; Eds.; The Royal Society of Chemistry: Cambridge, 1994.
42 J. Jr. Rebek, *Angew. Chem. Int. Ed. Engl.*, 1990, **29**, 245-255.
43 C. H. Hunter, K. R. Lawson, J. Perkins and C. J. Urch, *J. Chem. Soc., Perkin Trans.*, 2001, **2**, 651-669.

44 M. Nishio, M. Hirota and Y. Umezawa, The CH-π Interactions, Wiley-VCH, New York, 1998.
45 A. Dougherty, *Acc. Chem. Res.*, 2013, **46**, 885-893.
46 R. Pinalli, M. Suman and E. Dalcanale, *Eur. J. Org. Chem.*, 2004, **3**, 451-462.
47 R. De Zorzi, B. Dubessy, J.-C. Mulatier, S. Geremia, L. Randaccio and J.-P. Dutasta, *J. Org. Chem.*, 2007, **72**, 4528-4531.
48 R. M. Yebeutchou and E. Dalcanale, *J. Am. Chem. Soc.*, 2009, **131**, 2452-2453.
49 D. Menozzi, E. Biavardi, C. Massera, F. P. Schmidtchen, A. Cornia and E. Dalcanale, *Supramol. Chem.*, 2010, **22**, 768-775.
50 E. Biavardi, M. Favazza, A. Motta, I. L. Fragalà, C. Massera, L. Prodi, M. Montalti, M. Melegari, G. G. Condorelli and E. Dalcanale, *J. Am. Chem. Soc.*, 2009, **131**, 7447-7455.
51 M. Dionisio, G. Oliviero, D. Menozzi, S. Federici, R. M. Yebeutchou, F. P. Schmidtchen, E. Dalcanale and P. Bergese, *J. Am. Chem. Soc.*, 2012, **134**, 2392-1398.
52 E. Biavardi, S. Federici, C. Tudisco, D. Menozzi, C. Massera, A. Sottini, G. G. Condorelli, P. Bergese and E. Dalcanale, *Angew. Chem., Int. Ed.*, 2014, **53**, 9183-9188.
53 E. Biavardi, F. Ugozzoli and C. Massera, *Chem Commun.*, 2015, **51**, 3426-3429.
54 E. Biavardi, C. Tudisco, F. Maffei, A. Motta, C. Massera, G. G. Condorelli and E. Dalcanale, *Proc. Natl. Acad. Sci.*, 2012, **109**, 2263-2268.
55 R. Pinalli, G. Brancatelli, A. Pedrini, D. Menozzi, D. Hernández, P. Ballester, S. Geremia and E. Dalcanale, *J. Am. Chem. Soc.*, 2016, **8**, 8569−8580.
56 A. Sreekumar, L. M. Poisson, T. M. Rajendiran, A. P. Khan, Q. Cao, J. Yu, B. Laxman, R. Mehra, R. J. Lonigro, Y. Li, M. K. Nyati, A. Ahsan, S. Kalyana-Sundaram, B. Han, X. Cao, J. Byun, G. S. Omenn, D. Ghosh, S. Pennathur, D. C. Alexander, A. Berger, J. R. Shuster, J. T. Wei, S. Varambally, C. Beecher and A. M. Chinnaiyan, *Nature*, 2009, **457**, 910-914.
57 M. Dionisio, J. M. Schnorr, V. K. Michaelis, R. G. Griffin, T. M. Swager and E. Dalcanale, *J. Am. Chem. Soc.*, 2012, **134**, 6540-6543.
58 J. M. Schnorr and T. M.; Swager, *Chem. Mater.*, 2011, **23**, 646-657.
59 R. A. Potyrailo, C. Surman, N. Nagraj and A. Burns, *Chem. Rev.*, 2011, **111**, 7315-7354.
60 S. Liu, Q. Shen, Y. Cao, L. Gan, Z. Wang, M. L. Steigerwald and X. Guo, *Coord. Chem. Rev.*, 2010, **254**, 1101-1116.
61 E. Biavardi, G. Battistini, M. Montalti, R. M. Yebeutchou, L. Prodi and E. Dalcanale, *Chem. Commun.*, 2008, 1638-1640.
62 a) A. J. Bard, Electrogenerated Chemiluminescence, Marcel Dekker, New York, 2004; b) M. M. Richter, *Chem. Rev.*, 2004, **104**, 3003-3036.
63 G. Valenti, E Rampazzo, E. Biavardi, E. Villani, G. Fracasso, M. Marcaccio, F. Bertani, D. Ramarli, E. Dalcanale, F. Paolucci and L. Prodi, *Faraday Discuss.*, 2015, **185**, 299-309.
64 a) S. Lanouette, V. Mongeon, D. Figeys and J. F. Couture, *Mol. Syst. Biol.*, 2014, **10**, 724-750. b) S. M. Carlson and O. Gozani, *J. Mol. Biol.*, 2014, **426**, 3350-3362. c) H. Huang, S. Lin, B. A. Garcia and Y. Zhao, *Chem. Rev.*, 2015, **115**, 2376-2418.
65 Y. Liu, L. Perez, M. Mettry, C. J. Easley, R. J. Hooley and W. Zhong, *J. Am. Chem. Soc.*, 2016, **138**, 10746-10749.
66 S. M. Biros, E. C. Ullrich, F. Hof, L. Trembleau and J. Jr. Rebek, *J. Am. Chem. Soc.*, 2004, **126**, 2870−2876.
67 a) Y. Liu, P. Liao, Q. Cheng and R. J. Hooley, *J. Am. Chem. Soc.*, 2010, **132**, 10383-10390. b) Y.-J. Ghang, M. P. Schramm, F. Zhang, R. A. Acey, C. N. David, E. H. Wilson, Y. Wang, Q. Cheng and R. J. Hooley, *J. Am. Chem. Soc.*, 2013, **135**, 7090−7093. c) Y.-J. Ghang, J. J. Lloyd, M. P. Moehlig, J. K. Arguelles, M. Mettry, X. Zhang, R. R. Julian, Q. Cheng and R. J. Hooley, *Langmuir*, 2014, **30**, 10161−10166.
68 Y. Liu, L. Perez, A. D. Gill, M. Mettry, L. Li, Y. Wang, R. J. Hooley and W. Zhong, *J. Am. Chem. Soc.*, 2017, **139**, 10964-10967.
69 N. Bontempi, E. Biavardi, D. Bordiga, G. Candiani, I. Alessandri, P. Bergese and E. Dalcanale, *Nanoscale*, 2017, **9**, 8639-8646.
70 I. Alessandri, E. Biavardi, A. Gianoncelli, P. Bergese and E. Dalcanale, *ACS Appl. Mater. Interfaces*, 2016, **8**, 14944-14951.
71 S.H. Zeisel, *Annu. Rev. Nutr.*, 2006, **26**, 229-250.
72 G. Leitinger and P. J. Simmons, *J. Comp. Neurol.*, 2000, **416**, 345-355.
73 H. Fujii, Y. Ishiguro, E. Uchida and S. Yamamoto, *Nutr. Immunol.* 2008, **8**, 92-98.
74 R. Conde-Alvarez, M. J. Grillo, S. P. Salcedo, M. J. de Miguel, E. Fugier, J. P. Gorvel, I. Moriyon and M. Iriarte, *Cell. Microbiol.*, 2006, **8**, 1322-1335.
75 T. V.Barkhimer, J. R. Kirchhoff, R. A. Hudson, W. S. Messer and L. M. V. Tillekeratne, *Anal. Bioanal. Chem.*, 2008, **392**, 651-662.
76 M. Adamczyk, R. J. Brashear, P. G. Mattingly and P. H. Tsatsos, *Anal. Chim. Acta*, 2006, **579**, 61-67.
77 a) P. I. Holm, P. M. Ueland, G. Kvalheim and E. A. Lien, *Clin. Chem.*, 2003, **49**, 286-294. b) J. J. Zhang and Y. Zhu, *J. Chromatogr. A*, 2007, **1170**, 114-117. c) R. Dunphy and D. J Burinsky, *J. Pharm. Biomed. Anal.*, 2003, **31**, 905-15.
78 K.M. Mitchell, *Anal. Chem.*, 2004, **76**, 1098-1106.
79 J. Ampurdanés, G. A. Crespo, A. Maroto, M. A. Sarmentero, P. Ballester and F. X. Rius, *Biosens. Bioelectron.*, 2009, **25**, 344-349.
80 a) P. Ballester, A. Shivanyuk, A. R. Far and J. Jr. Rebek, *J. Am. Chem. Soc.*, 2002, **124**, 14014-14016. b) P. Ballester and M. A. Sarmentero, *Org. Lett.*, 2006, **8**, 3477-3480.
81 A. J. Michalska, C. Appaih-Kusi, L. Y. Heng, S. Walkiewicz and E. A. H. Hall, *Anal. Chem.*, 2004, **76**, 2031-2039.
82 J. Fritz, *Analyst*, 2008, **133**, 855-863.
83 P. Bergese, G. Oliviero, I. Alessandri and L.; Depero, *Colloid Interface Sci.*, 2007, **316**, 1017-1022.
84 K. Kotova, M. Hussain, G. Mustafa and P. A. Lieberzeit, *Sens. Actuators B* 2013, **189**, 199-202.
85 J. Lagona, P. Mukhopadhyay, S. Chakrabarti and L. Isaacs, *Angew Chem. Int. Ed.*, 2005, **44**, 4844-4870.
86 F. Biedermann, W. M. Nau and H.-J. Schneider, *Angew Chem. Int. Ed.*, 2014, **53**, 11158-11171.
87 G. Ghale and W. M. Nau, *Acc. Chem. Res.*, 2014, **47**, 2150-2159.
88 D. Lucas, T. Minami, G. Iannuzzi, L. Cao, J. B. Wittenberg, P. Anzenbacher Jr. and L. Isaacs, *J. Am. Chem. Soc.*, 2011, **133**, 17966-17976.
89 T. Minami, N. A. Esipenko, B. Zhang, M. E. Kozelkova, L. Isaacs, R. Nishiyabu, Y. Kubo and P. Anzenbacher Jr., *J. Am. Chem. Soc.*, 2012, **134**, 20021-20024.

90 M. del Pozo, P. Hernandez, L. Hernandez and C. Quintana, *J. Mater. Chem.*, 2011, **21**, 13657-13663.
91 M. Bush, N. Bouley and A. Urbach, *J. Am. Chem. Soc.*, 2005, **127**, 14511-14517.
92 P. Rajgariah and A. R. Urbach, *J. Inclusion Phenom. Macrocyclic Chem*., 2008, **62**, 251-254.
93 M. del Pozo, J. Mejías, P. Hernández and C. Quintana, *Sensors Actuat. B*, 2014, **193**, 62-69.
94 Y. Cao, D. Chen, W. Chen, J. Yu, Z. Chen and G. Li, *Anal. Chim. Acta*, 2014, **812**, 45-49.
95 D. Wang, Y. Yuan, Y. Zheng, Y. Chai and R. Yuan, *Chem.Commun.,* 2016, **52**, 5943-5945.
96 J. Zhao, H.-J. Kim, J. Oh, S.-Y. Kim, J. W. Lee, S. Makamoto, K. Yamaguchi and K. Kim, *Angew. Chem. Int. Ed.*, 2001, **40**, 4233-4235.
97 H. Kim, J. Oh, W. S. Jeon, N. Selvapalam, I. Hwang, Y. H. Ko and K. Kim, *Supramol. Chem.*, 2012, **24**, 487-491.
98 M. Jang, H. Kim, S. Lee, H. W. Kim, J. K. Khedkar, Y. M. Rhee, I. Hwang, K. Kim and J. H. Oh, *Adv. Funct. Mater.*, 2015, **25**, 4882-4888.
99 L. Torsi, M. Magliulo, K. Manoli and G. Palazzo, *Chem. Soc. Rev.*, 2013, **42**, 8612-8628.
100 M. E. Roberts, S. C. B. Mannsfeld, N. Queraltó, C. Reese, J. Locklin, W. Knoll and Z. Bao, *Proc. Natl. Acad. Sci. U.S.A.*, 2008, **105**, 12134-12139.
101 B. Kim, H. S. Song, H. J. Jin, E. J. Park, S. H. Lee, B. Y. Lee, T. H. Park and S. Hong, *Nano-technology*, 2013, **24**, 285501.
102 S. Ganapati, S. D. Grabitz, S. Murkli, F. Scheffenbichler, M. I. Rudolph, P. Y. Zavalij, M. Eikermann and L. Isaacs, *ChemBioChem*, 2017, **18**, 1583-1588.
103 E. G. Shcherbakova, B. Zhang, S. Gozem, T. Minami, P. Y. Zavalij, M. Pushina, L. Isaacs and P. Anzenbacher, Jr., *J. Am. Chem. Soc.*, 2017, **139**, 14954-14960.
104 T. Ogoshi, S. Kanai, S. Fujinami, T. A. Yamagishi and Y. Nakamoto, *J. Am. Chem. Soc.*, 2008, **130**, 5022-5023.
105 L.-L. Tan and Y.-W. Yang, *J. Incl. Phenom. Macrocycl. Chem.*, 2015, **81**, 13-33.
106 S. Dasgupta and P. S. Mukherjee, *Org. Biomol. Chem.*, 2017, **15**, 762-772.
107 C. W. Sathiyajith, R. R. Shaikh, Q. Han, Y. Zhang, K. Meguellati and Y.-W. Yang *ChemCommun.,* 2017, **53**, 677-696.
108 M. Bojtar, A. Paudics, D. Hessz, M. Kubinyi and I. Bitter, *RSC Adv.*, 2016, **6**, 86269–86275.
109 C.-W. Chen and H. W. Whitlock, *J. Am. Chem. Soc.*, 1978, **100**, 4921-4922.
110 T. Schrader, G. Bitan and F.-G. Klärner, *Chem. Commun.*, 2016, **52**, 11318-11334.
111 F.-G. Klärner and T. Schrader, *Acc. Chem. Res.*, 2013, **46**, 967-978.